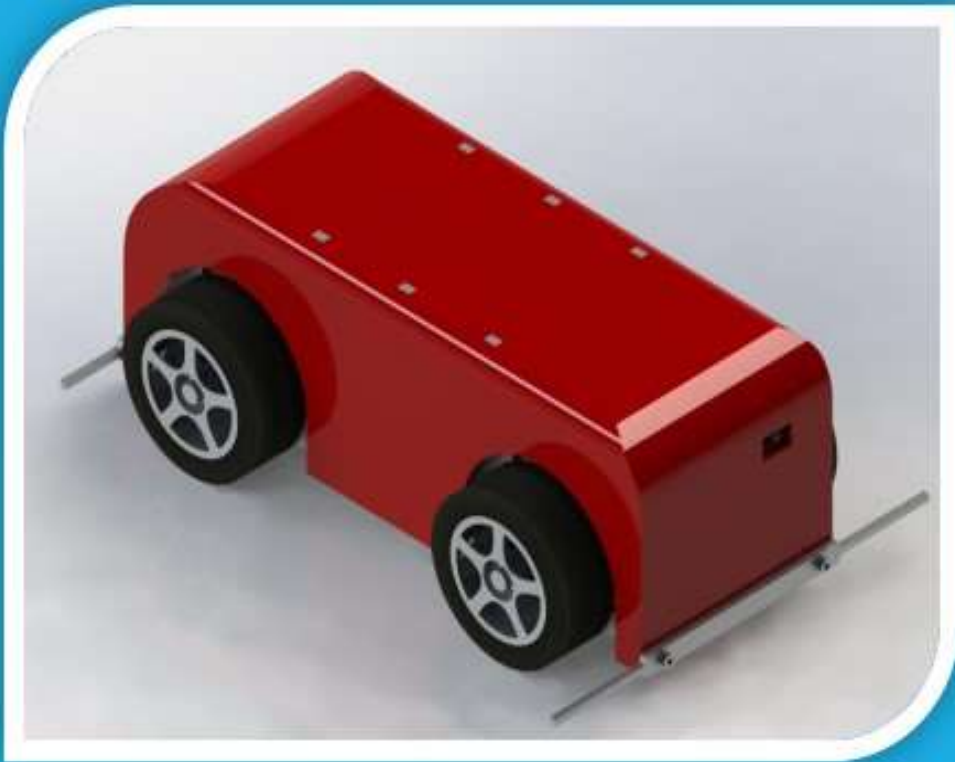


Imperial College
London



ME₂ AUTUMN DESIGN PROJECT: IDRIS' WHIP

Group P24

Asad Raja, Wenbo Chen, Nasir Islam, Rajiv
Samanta, Syed Ahamed

Executive Summary

This report details the completion of a project set by Imperial College London's Mechanical Engineering Department as part of the Second Year Design and Manufacture curriculum. We were tasked with the design and manufacture of a miniature motorised car, to be tested in speed, torque and loading challenges. The design had to be such that manufacturing could be conducted within the constraints of time, part availability and workshop machine capability. A 100-hour service life was also required. The car was to travel in a straight line and as such steering capabilities did not have to be implemented.

There were several stages and elements to the completion of this project, allowing each member of the group to develop skills in multiple areas. Effective project management and teamwork was key to the success of the project. We each also furthered our conceptual design, 3-D CAD modelling, engineering drawing communication, manufacturing and reporting skills.

Our car (Figure 1 and 2) is a four-wheel drive, two stage transmission solution to the task set, using bevel gears and a driveshaft. The driveshaft concept greatly informed the majority of our design and made our design elegant and simple yet unique and powerful. The concept was inspired by the drive transmission of real cars. Taking engineering inspiration from the real world and applying it to a specific design is an important skill for an engineer and we were pleased to be able to exercise it here.

This has been a very valuable experience for each of us as students of engineering and as individuals. Indeed, besides from the technical knowledge built upon, we have each improved upon our approach to project work, teamwork and report writing – skills that can be transferred to areas beyond just engineering. We would like to thank the department and Marc Mason for providing us this opportunity.

By the end of this project, we have produced the small motor car, this design report document, individual logbooks and a booklet recording project management decisions. At the time of writing this report, the final stages of manufacture are being completed. Upon assembly, our small motor car will be able to achieve a speed of approximately 1.9 m/s and a torque output of 0.2125 Nm.

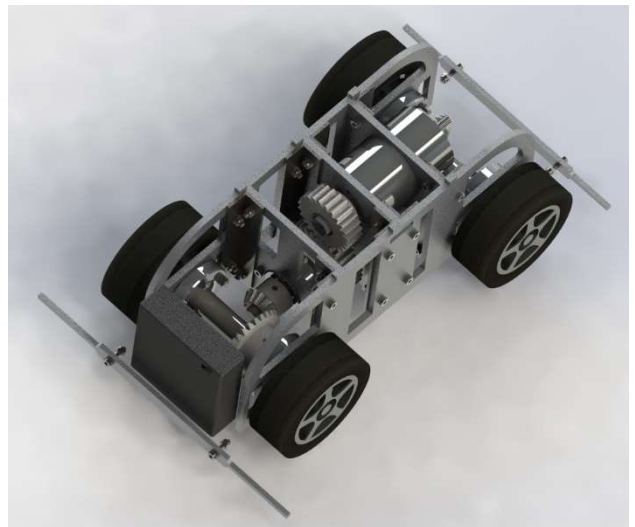


Figure 1 – Our car, shown with the cover removed

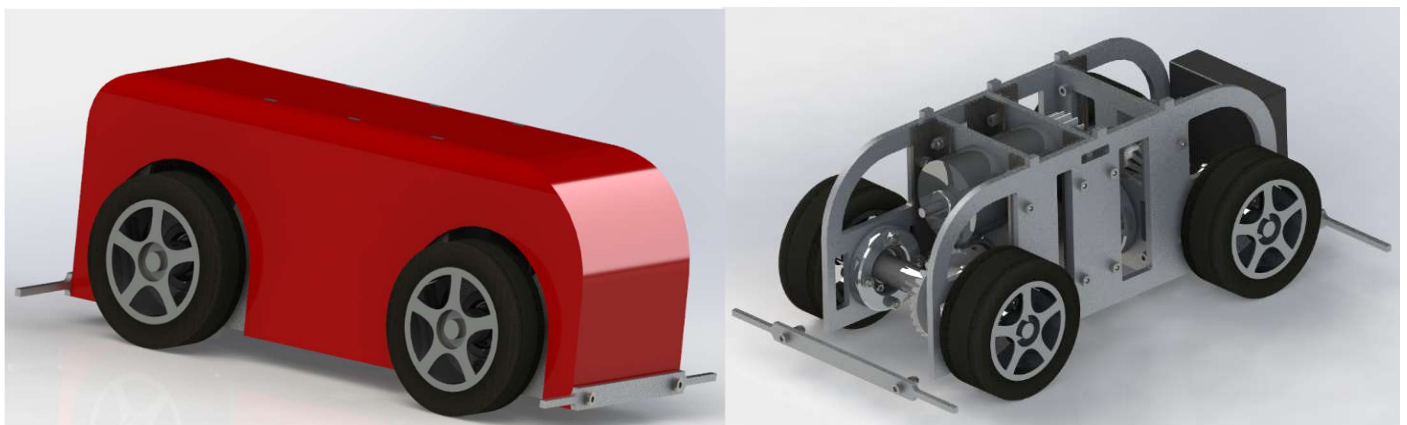


Figure 2 – Our car, shown with the cover (left) and with the cover removed (right)

Contents

Executive Summary	2
1. Introduction	4
2. Design Process	4
2.1. Product Design Specification	4
2.2. Gantt Chart	5
2.3. Initial Concepts	5
3. Breakdown of Final Design	7
3.1. Drive Transmission	7
3.2. Frame Design	8
3.3. Constraining	10
4. Analysis	12
4.1. Free Body Diagram Analysis	12
4.2. Gear Ratios	12
4.3. Lewis Equation and Bearing Analysis	13
4.4. Finite Element Analysis of the Side Plate	13
4.5. Driveshaft Analysis	13
4.6. Axle Shaft Analysis	14
5. Manufacturing Plan	15
5.1. Axle Shaft	16
5.2. Driveshaft	16
6. Conclusion	16
7. Inspection Report	17
8. Appendices	18
9. Engineering Drawings	20
9.1. Long Form Bill of Materials	20
9.2. Bearing Housing	21
9.3. Side Plate	22
9.4. Mid Plate	23
9.5. Driveshaft	24
9.6. Axle Shaft	25
9.7. Driveshaft Subassembly	26
9.8. Full Assembly	27

1. Introduction

Our mission statement for this project could be summarised, simply, as follows:

“Design and manufacture a small electric DC motor car to be tested in the three performance criteria of: speed torque and structural integrity.”

Though the deadline for manufacture of the car was 14th Dec 2018, these tests will be carried out on 6th Jun 2019. The tests include: a race against the vehicles of all other groups, a tug of war with other cars and a loading test of 80kg being applied to it. Other than performance during testing, our car would be assessed on safety, effectiveness of transmission and build quality. Each group were given the following components: a DC brushed motor, a battery pack, four AA batteries and four plastic wheels.

For the entirety of the project, our group employed a thorough, consistent and fervent work ethic. We also followed closely the department recommended design process, taking a methodical yet iterative approach (Figure 3).

From early on, the overarching aim of our design became minimising the number of parts to achieve simplicity (meaning that parts had to complete multiple functions) whilst also achieving a unique four-wheel drive system that will meet the necessary design criteria.

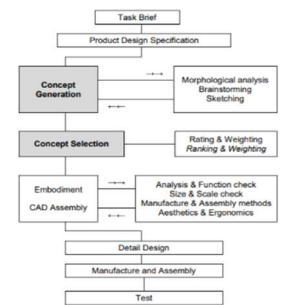


Figure 3 – Design Process (Gosling, 2017)

2. Design Process

2.1. Product Design Specification

Upon being given the project brief, the group decided that the best way to highlight the requirements of the brief was to form a product design specification document (Table 1). The PDS helped to provide some direction during the design phase whilst also giving the project an established grounding.

Table 1 – The product design specification

Product Design Specification		
Element	Criteria/Details	Verification
Production:		
Quantity	One vehicle to be produced.	Not applicable.
Manufacturing Budget	No budget (in moderation)	Reviewed during the choosing of components and materials.
Manufacturing Constraints	Limited time allowed for manufacturing (approximately 5 weeks). Laser cutting is subject to fair use policy. One part only to be CNC manufactured.	Reviewed during planning of the manufacturing process.
Manufacturing Methods	Laser Cutting, 3D Printer, Milling, Turning, Drilling, Lathe	Only these methods were used.
Parts and Components	Were able to order components from HPC Gears and RS Components. Materials were requested from the Imperial STW.	Not applicable.
Material	High strength to weight ratio, for a low vehicle weight (high acceleration) and structural strength.	Review and research during design process.
Regulatory:		
Safety	Plastic cover to avoid contact with moving parts. Sharp edges must be filed down.	Reviewed during design process.

Performance:		
Speed	Aiming to maximise this. Will depend on the transmission chosen, whether the car travels in a straight line and the friction present	To be tested after manufacturing through a short race.
Torque	Aiming to maximise this. Depends on the transmission chosen, and friction present.	To be tested after manufacturing through a 'tug of war' type challenge.
Structural Integrity	Aiming to allow the vehicle to comfortably handle an 80g vertical force applied on top. This will depend on the material chosen for the frame, the amount of material used, and the structure chosen.	To be tested after manufacturing by exerting an approximate force of 80g vertically on the vehicle.
Ergonomics and aesthetics	The power switch must be accessible from the outside of the vehicle. No loose parts are allowed, and the overall finish must be solid. Plastic cover is to hide inner structures.	Reviewed during design process.
Size:		
Width	Must be less than 20 cm to fit on the track. Aiming for a smaller vehicle, for a low weight.	Reviewed during design process.
Height	Aiming for a smaller vehicle, for a low weight.	Reviewed during design process.
Length	Aiming for a smaller vehicle, for a low weight.	Reviewed during design process.

2.2. Gantt Chart

The group also formalised a Gantt chart in order to ensure a timely project delivery, shown in Figure 4.

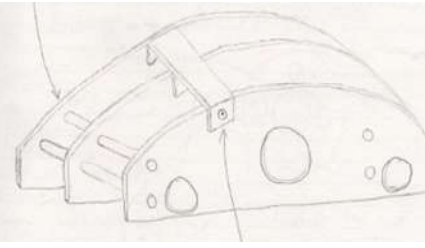
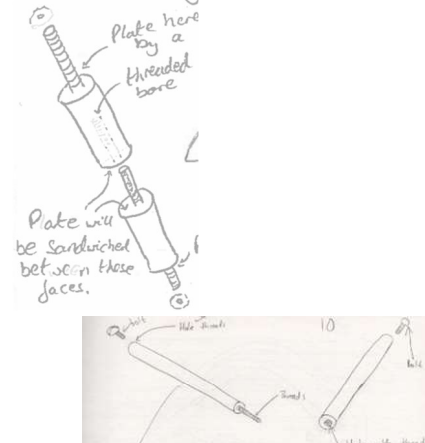
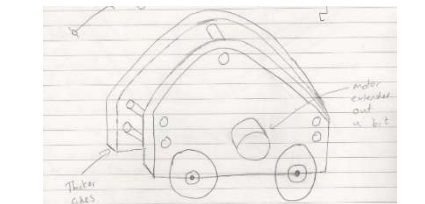
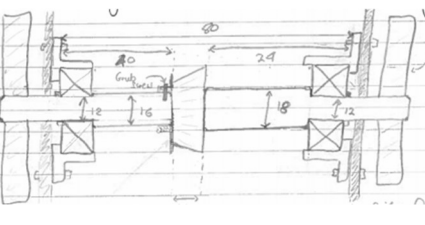
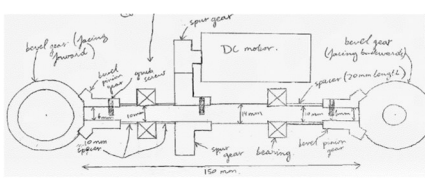


Figure 4 – Gantt chart (an A4 size Gantt Chart is included in the project management booklet)

2.3. Initial Concepts

Table 2 – A table summarising concept generation in the brainstorming phase

Idea Considered	Sketches	Explanation and Evaluation
Belt Transmission		Early on, single stage transmission and two-wheel drive systems were rejected since satisfactory drive ratios could not be achieved without making the car bulky or unbalanced. The drive systems we consequently considered mostly involved belts. We decided against such a system since belts are less efficient at transmitting torque, can slip and required the use of tensioners thus reducing simplicity. The use of a driveshaft required less parts whilst achieving the same results.

<p>A single mid plate parallel to the side plates</p>		<p>This design would have required the motor to be face mounted against the middle plate with a cut out in one of the side plates to allow for the extended length of the motor. However, when the driveshaft transmission system was decided upon, this became redundant since the motor was to sit parallel to the car.</p>
<p>Supporting Rods</p>		<p>The purpose of these rods was to join parallel plates to provide structural rigidity. The rods would have screwed into each other, sandwiching a plate, with a tapped hole in either end for a bolt to screw into, securing the other two plates. However, they were decided against since they would have been difficult to manufacture, and the weight gain would have been greater than the improvement in strength. Furthermore, the motor partly achieved the function of these supporting rods by intersecting two plates in our final drive transmission idea.</p>
<p>Thicker Plates</p>		<p>Using a shorter chassis and having thicker plates was thought to have had an advantage in there being less bending during a step test. However, this idea was abandoned as having a shorter chassis would have made the car more prone to turning during motion. Furthermore, the plate thickness was limited to 4mm by the cutting capacity of the laser cutter.</p>
<p>Alternative Constraining of Bearings</p>		<p>We had previously considered a system whereby each bearing had the outer race constrained in one direction and the inner race constrained in both directions. However, we were advised that, for every bearing pair, it is better practice to constrain only one race of one of the bearings in both directions but both races of the other bearing in both directions as this allows movement of the bearing with heat fluctuations.</p>
<p>Spacers</p>		<p>We also considered the use of spacers to axially constrain components but, since these were not readily available to us, we would have had to manufacture them which would have been time consuming.</p>

Having considered a range of alternatives in relations to the drive transmission, chassis and constraining of components, we began to solidify what would become our final design (Figure 5a and 5b). For the remainder of the project, this remained the general concept of our design.

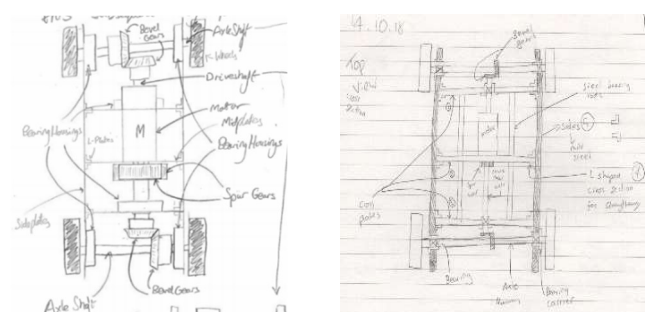


Figure 5a (left) and 5b (right) – Two sketches of our selected design following the concept generation phase

3. Breakdown of Final Design

3.1. Drive Transmission

The drive transmission used in our design is a four-wheel drive, two stage transmission consisting of Delrin spur gears and bevel gears (Figure 6). It was chosen to succeed in the tests we were assigned (according to the specifications laid out in our PDS) by maximising power output from the motor and do so in a balanced, compact and efficient manner.

How it works

The overall transmission is as presented in Figure 6. The first torque amplification is between the motor and the driveshaft via spur gears. There is then a second torque amplification between the driveshaft and both axles via bevel gears. The overall torque amplification of the transmission is 2.5x. The calculations for transmission ratios are provided in Appendix 1.

Stage 1 transmission uses spur gears from the motor shaft to the driveshaft as both are positioned centrally along the length of the car (Figure 7a). Due to the very short length of the motor shaft, the spur gear on it is pushed as close to the motor as possible without interfering with other parts. The spur gear on the driveshaft is positioned roughly halfway along its length allowing the bevel gears for stage 2 to be positioned on the ends. The motor shaft gear has a PCD of 36 mm whilst the driveshaft gear has a PCD of 45 mm resulting in a torque amplification of 1.25x for this stage. Each gear has a module of 1.5 mm.

Stage 2 transmission uses bevel gears from the driveshaft to the axles to reorient the rotational motion along the length of the car to rotational motion along the width of it (Figure 7b). The bevel gears on each axle are positioned oppositely to ensure they spin together in the correct direction. The driveshaft bevel gears have PCDs of 22.5 mm whilst the axle bevel gears have PCDs of 45 mm resulting in a torque amplification of 2x for this stage. Each gear has a module of 1.5 mm.

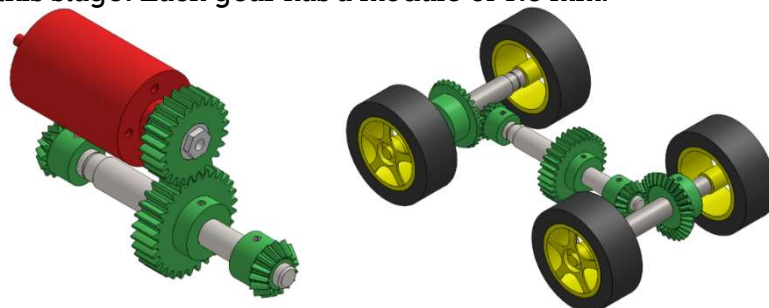


Figure 7a (left) and Figure 7b (right) – Stage 1 and stage 2 transmissions

Why we chose it

The reason we chose a four-wheel drive system was because we wanted to get as much traction on the ground as possible. We reasoned that, due to the likely low coefficient of friction of the floor the tests would be conducted on, it would be beneficial to have the power distributed to all wheels so that in the event of a wheel slipping, only 25% of our power would be affected as opposed to potentially 50%. It was also hoped that this would further help keep our car travelling as straight as possible.

Another primary reason for choosing this design was to keep the weight distribution across the width of the car as even as possible. This was important to us as we reasoned that if there was uneven distribution, some wheels would have more traction than others and this could cause the car to veer into the racetrack walls and lose power due to friction.

The use of a driveshaft allowed us to place the motor lengthwise along the vehicle as well as having the axle bevel gears also fairly central. Therefore, the vast majority of the weight was balanced and any small variations we hoped would not make a significant impact.

The design choice of having a two-stage transmission was because we wanted a significant torque amplification whilst still maintaining a compact system. Furthermore, our goal of even weight distribution

coupled with the choice of using four-wheel drive meant single stage transmission was not possible. The necessity of bevel gears on the axles also led to spatial constraints that single stage transmission could not comfortably satisfy whilst giving us the gear ratios we required.

Our use of gears was because of their highly efficient operation and relative simplicity. Gears are not subject to the slipping issues present with a belt transmission and are simpler and more reliable than a chain drive. A potential issue identified with gears was their greater weight.

How it was adapted

Although the general transmission design did not change much during the design process, one major change was from steel to Delrin gears. The initial design did in fact use plastic gears to save weight, but the original parts supplier did not have them in the PCDs we required so we settled for steel. However, in rough weight calculations done in Solidworks after modelling, we discovered that the weight of the car was too large and risked stalling the motor. Fortunately, by this point a new parts supplier had become available from which a wide range of plastic gears could be purchased. We were able to then switch out the steel gears for Delrin gears with minimal impact to the rest of the design but a massive weight saving of approximately 0.5 kg.

3.2. Frame Design

The chassis serves as the main structure that houses all components other than the wheels (the entire transmission system including the motor, the bearing housings and the power pack). It serves to provide support, structure and robustness to the car.

How it works

The whole frame is made up of two identical side plates and three unique mid plates in between, placed perpendicular to the side-plates (Figure 8 and 9). All plates are 4 mm thick and laser cut from aluminium. The three mid plates have small rectangular cut-outs in each of their corners which creates a tenon. Grooves were cut in each of the side plates allowing these mid-plates to slot in easily to the side plates. In addition to these grooves and tenons, the mid-plates and side plates are joined with L-brackets to prevent twisting and torsion of the chassis. The front and back mid-plates have only one L-bracket on each side (outward facing) whereas the middle mid-plate has two on each side. These brackets are attached by M3 nuts and bolts with clearance holes drilled in the relevant positions.

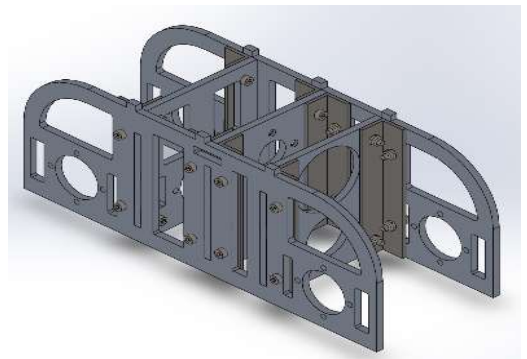


Figure 8 – The full chassis

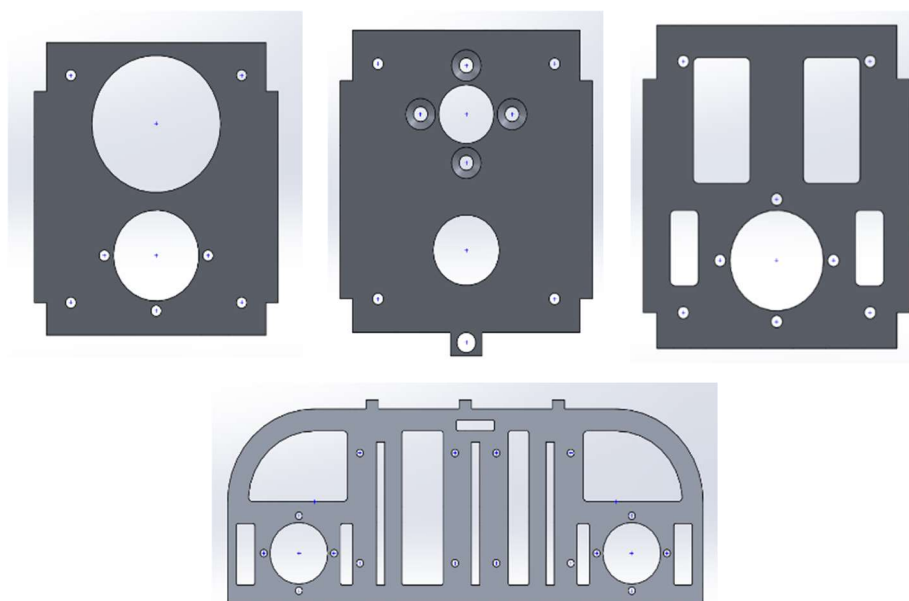


Figure 9 – The back mid plate, middle mid plate, front mid plate and side plate (clockwise)

Each of the three mid-plates have a hole in the lower half to accommodate the driveshaft. These holes in the front and back mid-plate hold bearing housings whereas in the middle mid-plate, it simply acts as a clearance hole for the driveshaft to pass through. The middle mid-plate also has a hole in its upper half for the motor shaft's hub, with four M4 countersunk holes drilled around it to allow face mounting of the motor. There is also a round cut-out in the back mid plate for the motor to sit in as it was too long to clear this. The side-plates and the front and back mid-plates have holes for the bearing carriers with four clearance M3 holes around it to allow attachment of the carriers. The middle mid-plate has a small notch at the bottom which an M4 hole so that the eyebolt can be attached and easily accessed.

Why we chose it

One of the requirements of this project is that the chassis must support a weight of around 80 kg which is the weight of average man. This was noted early in the design stage as a crucial factor to the design. Aluminium was therefore selected for the chassis plates due to its greater ductility than steel. It also has a lower density, keeping the plates light and helping to meet our mass target of 1.9 kg (Section 4.2) in order to achieve maximum power output of the electric motor. Aluminium is also easier to work on compared to steel due to its softer, more malleable nature which is advantageous if some adjustment of components was needed (e.g. filing or hacksawing).

With our design of bevel and spur gears, our alignment had to be perfect so that the gears meshed properly and would run together smoothly without misalignment. The grooves and tenons for the interlocking of the plates was used to ensure this, keeping the mid plates and side plates of our chassis at right angles to one another.

Our decision to use three mid plates was due to our choice of drive transmission. With a driveshaft positioned along the length of the car, a bearing was required to support it near either of its ends. Therefore, a mid plate was required both near the front and back of the car, with a bearing housing attached to each. A middle mid plate was also required so as to mount the motor in the position specified by our chosen drive transmission. Using three mid plates also had the added benefit of the frame providing extra support to the motor which is quite bulky and heavy.

The whole frame is put together using M3 nuts and bolts as tapping 28 holes would have been time consuming and more difficult to manufacture. This way, the frame was easier to build and to disassemble if needed. Countersunk screw holes were used for motor mounting in the middle mid plate so that the screw heads would not touch the spur gear attached to the motor shaft. The notch where the eyebolt is placed was chosen to be on the middle mid-plate as it would minimise the moment in the tug of war contest and allows the weight distribution to remain equal and prevent flipping of the car.

Cut-outs are also employed in the side plates and mid plates to allow weight saving so that our target weight could be met. The corners in the cut-outs were filleted to reduce stress concentrations. Using Finite Element Analysis in Solidworks, it was found that fillet radii of over 2 mm were sufficient. The side-plates and the mid-plates were laser cut to ensure ease of manufacture and a greater tolerance than would have been achievable through manual manufacture (+/- 0.1 mm). The tolerancing of the plates was crucial since it reduced the risk of misalignment of the bearings and gears.

The side-plates and L-brackets were designed to be identical to increase the ease and speed of manufacture.

How it was adapted

Assigning the relevant material densities to each part in the assembly, we used Finite Element Analysis to find that the car weighed over 3 kg. This meant that we were at risk of exceeding the stall torque meaning the car would not move. Therefore, weight needed to be reduced. As well as swapping the steel gears for plastic, this was done by cutting additional material out of the plates.

When it came to manufacture of the L-brackets, which were made from bending 2 mm aluminium plates into an L-shape, it was found that the aluminium would crack along the bend edge. Heat treatment in the form of annealing was therefore conducted before bending to alleviate stresses and remove dislocations, making the material more malleable to bending.

3.3. Constraining

The constraining referred to in this section can be categorised into that of the bearings, the gears and the wheels. Effective constraining of each of these parts is the means by which the drive transmission concept is realised.

How it works

Our design contains six bearings in total – two on each of the identical axle shafts and two on the driveshaft. Each pair of bearings is constrained in an identical way. For one bearing, the external race is constrained in both directions by features of its bearing housing, using a step-down on one side of the bearing and an internal circlip on the other. For the other bearing, the external race is constrained in the same way, but the internal race is also constrained in both directions, with a step-up in the shaft on one side and an external circlip on the other. Each part of the shaft where the inner race of a bearing sits is manufactured to a j5 tolerance (+0.005 / -0.003 mm) and each part of the bearing housing where the external race of a bearing sits is manufactured to a H7 tolerance (+0.021 / 0.000 mm).

There are two spur gears in our design, one on the motor shaft (the pinion) and one on the driveshaft. There are also four bevel gears, one on either end of the driveshaft (the pinions) and one on either axle shaft. The spur gear located on the motor shaft is constrained using a keyless bush. This constrains the gear both radially and axially and demands no modification of the motor shaft. Each of the other five gears are constrained with an M4 grub screw and a step-up of the shaft on one side of it. The grub screws constrain the gears both radially and axially though the step-up of the shaft achieves some additional axial constraining in one direction. Flats are milled onto each point of each shaft where a grub screw sits to aid torque transmission and prevent slipping.

The wheels we were given had an irregular bore profile. As shown by Figures 10a and 10b, these bores were rectangular but with circular width edges of the dimensions specified.

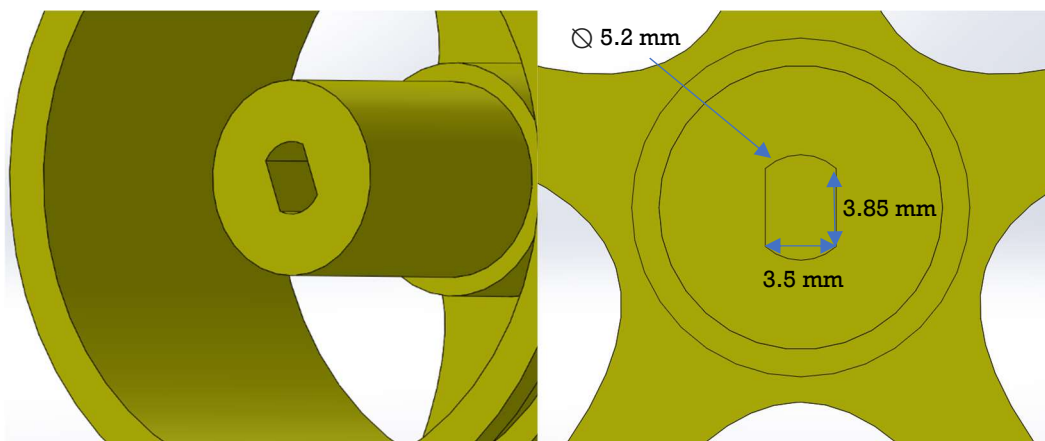


Figure 10a (left) and Figure 10b (right) – Wheel hub bore profile

To constrain these wheels to the axle shafts, we drilled and reamed an 8 mm hole in the hub (hence removing the straight edges of the bore profile). Turning the end of the axle shafts to this same dimension and then knurling these sections, an interference fit is used to constrain the wheels both radially and axially. The shaft ends were knurled so as to ensure torque transmission by increasing the friction between the rotating shaft and the inside of the wheel hub. In fact, knurling the shaft end increased the diameter of these sections slightly, meaning when they are hydraulically pressed into the wheel hubs to interference fit them, the knurled surface cuts into the plastic bore profile slightly, ensuring strong torque transmission.

Why we chose it

Our constraining choices were informed by our goal of design simplicity. For example, the keyless bush, grub screws and interference fit of the wheels each achieved both axial and radial constraining. This, as well as the fact that half of all bearing constraining was achieved with steps in our shafts, meant that the number of components required for constraining was minimised. The shaft steps for our gears also accomplished a double function in that they not only provided extra axial constraining in one direction, but also allowed us to position our gears accurately.

Simplicity was also achieved by constraining the bearings in such a way that the bearing housings are identical. We were also confident in using circlips in our constraining since they are suitable for relatively low axial force applications such as this one.

The choice of a keyless bush to constrain the spur gear on our motor shaft as opposed to a grub screw was due to a keyless bush requiring no modification of the motor shaft. Modification of the motor shaft (e.g. to turn a circlip groove or shoulder or to mill a keyway or a flat for a grub screw) may have caused damage to the motor or fracture of the shaft itself which had a diameter of only 5 mm. A concern with this method of constraining when it came to the embodiment of our design was that, as shown by Figure 11, the motor shaft could only be fitted into a fraction of the keyless bush's total length (6.25 mm to be exact). This was due to the limited length of the motor shaft. Our concern was that the lack of area over which the torsional force of the motor shaft acts within the keyless bush would result in high shear forces being introduced here, potentially causing slippage. Nevertheless, we calculated the shear stress in the keyless bush to be 346.3 kPa in this situation (Appendix A1), which is less than the maximum allowable shear stress of steel (200 MPa) and therefore acceptable.

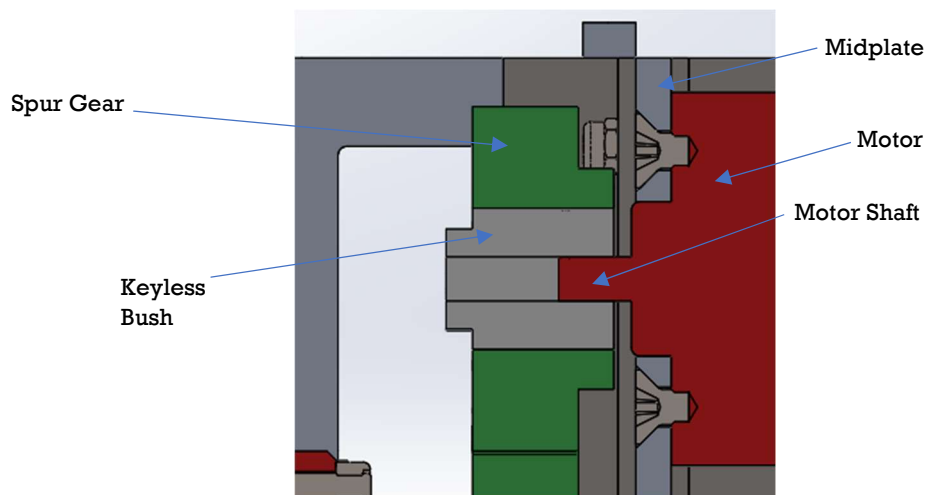


Figure 11 – A section view of the car showing the keyless bush constraining the spur gear on the motor shaft.

Though the use of grub screws for the constraining of all our other gears was slightly contentious due to their relatively low torque capacity, we were able to confirm their suitability since, for our application of an M4 grub screw on mild steel, their torsional holding capacity was found to be approximately 2.3 Nm (Appendix A2). Since the maximum torque experienced in our drive transmission system is 0.21 Nm, grub screws suffice for the constraining of the gears. The use of grub screws as opposed to a reasonable alternative such as keys saved us a lot of manufacturing time since milling flats onto our shafts was a far quicker process than having to mill a precise keyway slot and manufacture a key. Since manufacturing time was limited, this decision proved highly advantageous.

Similarly, the constraining of the wheels with a knurled-shaft interference fit also reduced manufacturing time as knurling is a quick and simple process. Indeed, we had previously considered a far more time-consuming process for constraining the wheels – that being the milling of the axle shaft ends after they had been turned to a 5.2 mm diameter in order to create flat parts on either side of the shaft, 3.5 mm apart. In this way we had planned to create a profile identical to that of the wheel hub bore shown in Figure 10b. A non-knurled shaft interference fit was also briefly considered but clearly this would have been a poor transmitter of torque.

How it was adapted

Originally, we had created our Solidworks assembly using internal circlips of diameter 21 mm to constrain the bearings. This was a misstep on our part since this circlip size was not available to us. The closest size available was the 24mm diameter internal circlip, and we therefore made necessary adjustments in our bearing carriers to make this substitution in the assembly. However, when doing this it was found that the bearing carrier on the back mid plate would interfere with the motor due to its increased diameter. To overcome this, we decided that the top of this bearing carrier should be hacksawed off, attaching it to the plate with three screws instead of four.

4. Analysis

4.1. Free Body Diagram Analysis

The schematic diagram shown in Figure 12a describes the basic dynamic situation at one wheel of the car when moving at a steady velocity. This has been split into separate free body diagrams of the wheel and ground in Figure 12b. As shown, the forces acting on the wheel are the frictional and reaction forces of the ground and the weight of part of the car. The frictional force is what drives the car. This is generated by the equal and opposite turning force corresponding to the wheel's torque output (by Newton's Third Law).

Therefore, analysing the free body diagram of one wheel would allow us to compute the output torque of one wheel from the turning force. Clearly, multiplying this by four would then give us the total required torque output of the car, which we were then able to use in our gear calculations. As shown by Appendix B1, our car's total torque output was found to be 0.223 Nm when a total mass of 2 kg was presumed. Setting a gear ratio that corresponded to maximum power output for this output torque in the motor, 2 kg became our initial target car mass that would allow us to achieve maximum speed at this output torque (maximum motor power). Naturally, the gear sizes available did not allow for a gear ratio that would output exactly 0.223 Nm, so there was subsequently a slight adjustment in our target total mass as detailed in the next section.

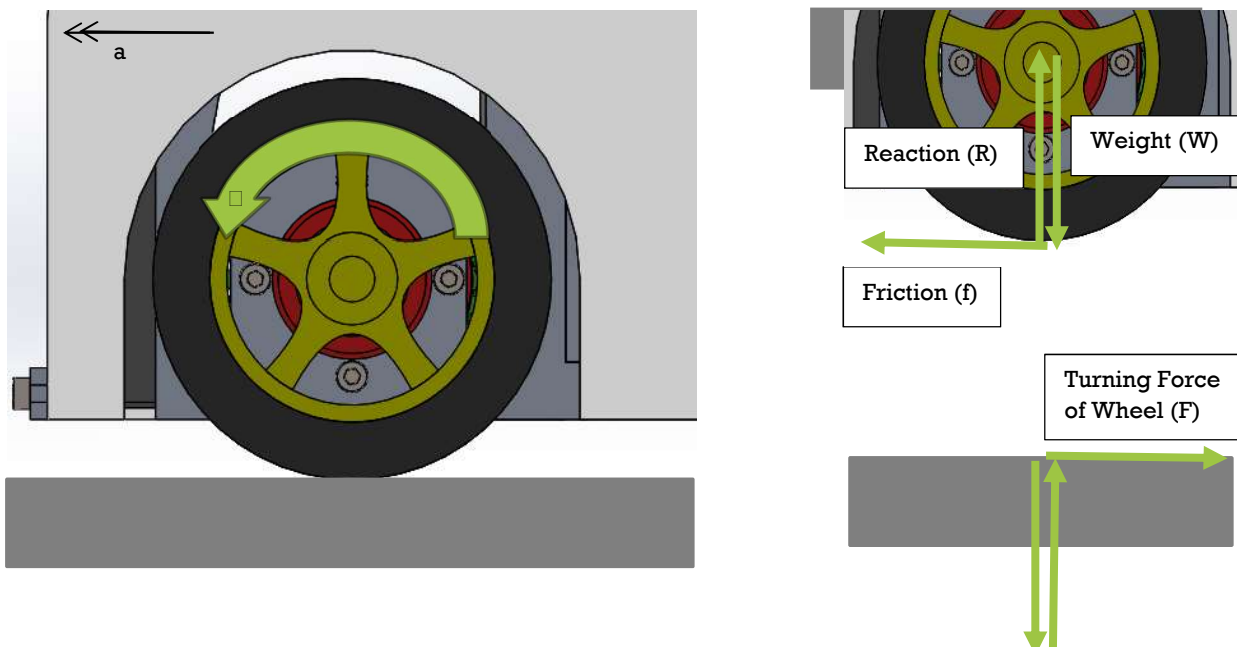


Figure 12a (left) and 12b (right) – A schematic of the wheel during motion and a free body diagram for the wheel and ground.

4.2. Gear Ratios

As detailed in Appendix B2, the final gear ratio we decided to use gave an overall torque amplification of 2.5x with 1.25x coming from stage 1 of the transmission and 2x coming from stage 2. This introduced a target car mass of 1.9 kg which would correspond with maximum motor power output, allowing the car to reach a speed of 1.91 m/s at a torque of 0.2125 Nm.

4.3. Lewis Equation and Bearing Analysis

Using the Lewis Equation as shown in Appendix C1, the gears were found to have respective minimum face width values of $w_{spur}=0.325$ mm and $w_{bevel}=0.685$ mm. Since the gears selected each have a larger face width value than these minimum values, they can withstand the forces through the transmission stages.

The calculated minimum dynamic load rating, C_{min} , for the bearings to last the required 100 hours of service life is $C_{min}=659.43$ N (Appendix C2). This meant we could use SKF-61901 bearings, since their value for C is 2.91 kN, higher than the minimum.

4.4. Finite Element Analysis of the Side Plate

Setting a mesh of 1.5 mm and material properties of aluminium 6082 T6, Solidworks Finite Element Analysis was conducted on the side plate to ensure that there would not be excessive stresses present that would cause it to fail. The force acting on the plate was assumed to be a distributed load of 800 N, which allowed for a conservative estimate of stresses since it is unlikely that the entire weight of the person standing on it will act on only one plate (as opposed to being distributed more evenly across the whole top of the frame).

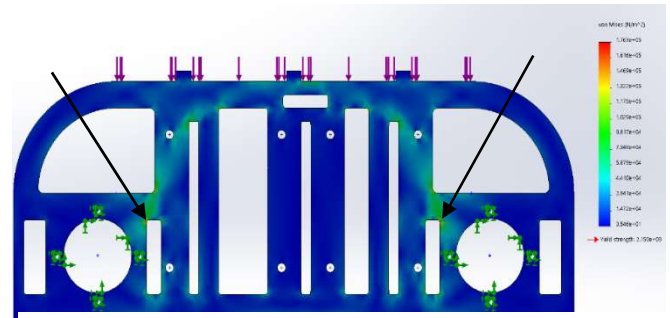


Figure 13 – a Finite Element Analysis of the side plate showing values of stresses at different points.

From Figure 13, we can see that most of the side-plate is blue which means that stress is low and is much lower than the yield stress (215 MPa). There are only two points that are red which are indicated by the two arrows, although stresses here are 1.763×10^5 N/m² which is still much lower than yield stress.

4.5. Driveshaft Analysis

On the judgement of our design tutor, the driveshaft was modelled as a beam simply supported on each end A and B by the bevel gears (Figure 14). The 80 kg weight was represented as two point-loads with each bearing transferring a load of $40g$ each. This is a slight overestimation since it represents a situation where no weight acts through the axle shafts. Note that in both shaft calculations that follow, the mass of the gears (approximately 0.03 kg) and the shafts (approximately 0.2 kg) were taken as negligible compared to the 80kg weight and so were disregarded to simplify the calculations.

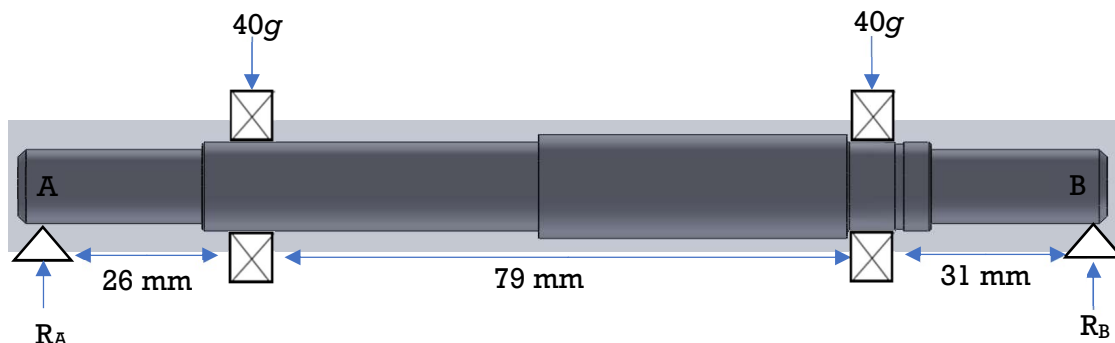


Figure 14 – the free body diagram used for analysis of the driveshaft

Summing the forces vertically and taking moments about point A, the reaction forces from the bevel gears were found to be $R_A=407.83$ N and $R_B=377.97$ N. Now, using the Macaulay method, an expression for the bending moment (BM) was formed:

$$BM(x) = -R_A x + 40g \langle x - 0.026 \rangle + 40g \langle x - 0.105 \rangle \quad (1)$$

From Figure 15, the maximum bending moment occurs at $x=0.105$ m and is equal to: $BM_{max} = -11.82$ Nm. From this, the maximum stress, σ_{max} , was then calculated, taking r to be the shaft's minimum radius of 5 mm:

$$\sigma_{max} = \frac{BM_{max} \times y_{max}}{I} = \frac{BM_{max} \times r}{\frac{\pi r^4}{4}} = \frac{11.82 \times 0.005}{\frac{\pi \times 0.006^4}{4}} = 120.4 \text{ MPa} \quad (2)$$

Despite this result being an overestimation as mentioned previously, this stress is significantly less than the yield stress, σ_{yield} , of mild steel (240 MPa). The safety factor (SF) implied by this result was calculated as follows:

$$SF = \frac{\sigma_{yield}}{\sigma_{max}} = \frac{240}{120.4} = 2.00 \quad (3)$$

Considering this result, we are confident that the driveshaft will not undergo any plastic deformation under the loading conditions and thus its operation after loading will not be affected.

Finally, to ensure the bearings are not misaligned heavily during the load test, the deflection, v , was calculated and compared to the maximum allowed deflection (v_{max}) of 0.13 mm (Mason, 2018). The bending moment equation was integrated twice, and Equation 4 was formed:

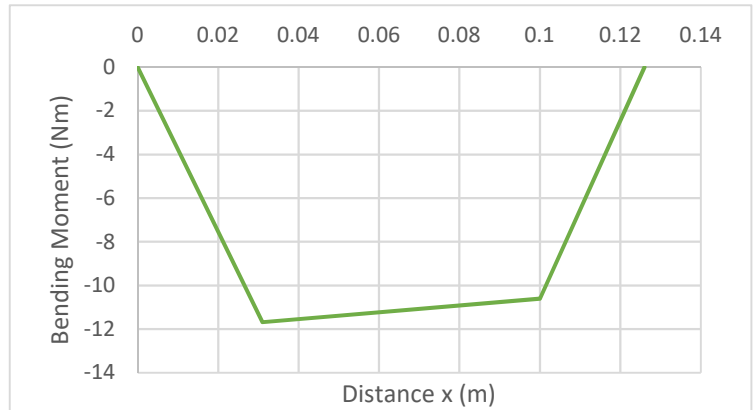


Figure 15 – A graph showing the bending moment against distance x , along the driveshaft length

$$EIv(x) = \frac{-R_A x^3 + 40g \langle x - 0.026 \rangle^3 + 40g \langle x - 0.105 \rangle^3}{6} + Cx + D \quad (4)$$

Using the boundary conditions $v(0) = v(0.136) = 0$, the values for the constants were found to be $C=0.603$ and $D=0$

With a mild steel Young’s Modulus value of $E=207 \text{ GPa}$ and a shaft radius of $r=6 \text{ mm}$ (for the radius of the shaft at the bearing positions), we were able to simply substitute the relevant x values into Equation 4 to obtain the bearing deflections:

Table 3 – The deflection of the two bearings under static loading

Bearing (as seen in Figure 14)	x position (m)	Deflection v (mm)
Left	0.026	0.069
Right	0.105	0.080

Since these were all under 0.13 mm, the bearings were found to not undergo any significant misalignment during both the static load test and operation (where loading would be significantly less).

4.6. Axle Shaft Analysis

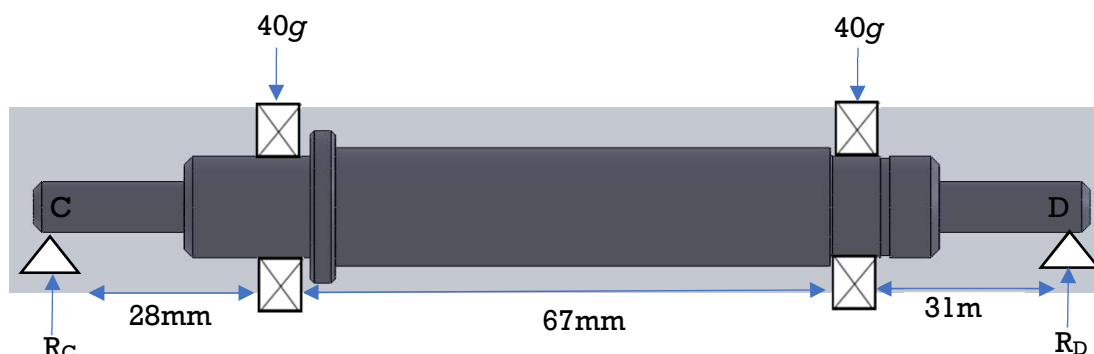


Figure 16 – the free body diagram used for analysis on the axle shafts

The axle shafts were modelled as being under a 40g load applied to each bearing with the normal reaction forces being produced by the wheels (Figure 16). In reality, the 80g will be spread over the two axle shafts and so these calculations are an overestimate of the value in order to account for any assumptions.

Summing forces vertically and taking moments from point C, the values for the reaction forces were found to be $R_C=401.74$ N and $R_D=383.06$ N.

Next, using Macaulay's method, Equation 5 for the bending moments, BM was formed:

$$BM(x) = -R_C x + 40g \langle x - 0.028 \rangle + 40g \langle x - 0.095 \rangle \quad (5)$$

Plotting the bending moment diagram (Figure 17) it can be seen that the maximum bending occurs at $x=0.095$ m which gave a maximum bending moment, $BM_{max} = -11.87$ N.

This result was used to calculate σ_{max} , taking r to be the shafts minimum radius of 4 mm:

$$\sigma_{max} = \frac{BM_{max} \times y_{max}}{I} = \frac{BM_{max} \times r}{\frac{\pi r^4}{4}} = \frac{11.87 \times 0.004}{\frac{\pi \times 0.004^4}{4}} = 236.15 \text{ MPa} \quad (6)$$

Though this result is a clear overestimate as one axle shaft alone will not experience the full $80g$ force, the stress value is still less than the yield stress of mild steel, $\sigma_{yield}=240$ MPa. This implies that the axle shaft certainly will not plastically deform after the static load test and will return back to its original shape ready to run despite the seemingly low safety factor demonstrated by these calculations.

Again, to ensure the bearings are not misaligned heavily during the load test, the deflection in the shaft was calculated and compared to the maximum allowed deflection of $v_{max}=0.13$ mm (Mason, 2018). Equation 5 was integrated twice, and the following was obtained:

$$EIv(x) = \frac{-R_C x^3 + 40g \langle x - 0.028 \rangle^3 + 40g \langle x - 0.095 \rangle^3}{6} + Ax + B \quad (7)$$

Using the boundary conditions from the reaction points, $v(0) = v(0.126) = 0$, the values for the constants were found to be $A=0.559$ and $B=0$.

Using a mild steel Young's Modulus value of $E=207$ GPa and a shaft radius of $r=6$ mm (the radius value for the parts of the shaft where the bearings sit), we found:

$$EI = E \frac{\pi r^4}{4} = 207 \times 10^9 \times \frac{\pi \times 0.006^4}{4} = 210.7 \quad (8)$$

Inputting this into Equation 7 at the relevant x values, we found the deflection in our bearings to be:

Table 4 – The deflection of the two bearings under static loading

Bearing (as seen in Figure 16)	x position (m)	Deflection v (mm)
Left	0.028	0.067
Right	0.095	0.073

Clearly, the bearings will not undergo any significant misalignment as each value is considerably less than the quoted maximum allowable deflection of 0.13 mm.

5. Manufacturing Plan

The parts that required manufacturing were the L-brackets, the driveshaft and the two identical axle shafts. All the chassis plates were laser cut and the cover of the car was 3-D printed. The six bearing carriers were CNC turned. Minor modifications were also required on most non-manufactured parts. For

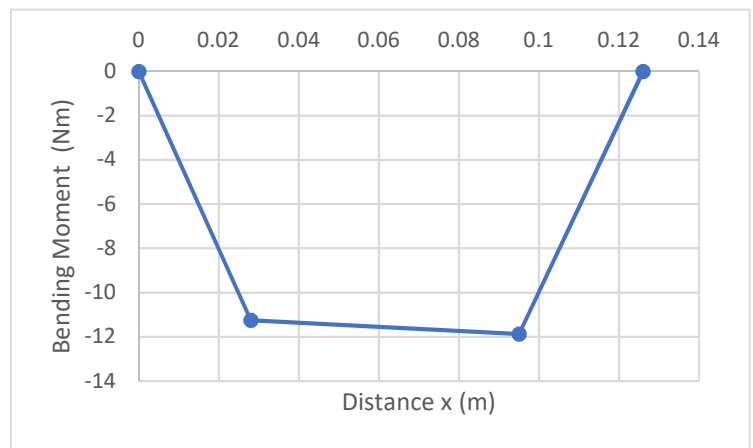


Figure 17 – A graph showing the bending moment against distance x , along the axle shaft length

example, bores and holes of relevant sizes were milled and drilled into the wheels, chassis plates, bearing housings and gears.

5.1. Axle Shaft

The axle shaft was mainly manufactured on a lathe by turning it with various cutting tools, then finished on a mill to add the flats for the grub screws.

To begin with, a cylinder of diameter 20 mm and length of around 170 mm was cut using a bandsaw. This diameter clearance allowed us to control every dimension radially and the length clearance gave us dimensional control axially as well as allowing us to grip the part in the lathe comfortably. A centre hole was also added to the free end that allowed further gripping with a lathe centre to keep the part aligned down its axis.

The free end of the shaft was then faced off and the Z axis zeroed here. The left side of the axle (from the 18 mm diameter shoulder as orientated in our engineering drawing) was then turned down in increments of 0.5 mm to the required dimensions. For diameters requiring more precise tolerances, as we neared the diameter needed, we recalibrated the X axis of the lathe after every cut by measuring the new cut diameter with a micrometer. Once the main cuts were completed, the cutting tool was replaced with a chamfer tool for the 1 mm chamfers, then a knurling tool to create the knurl on the end of the shaft. Then a circlip groove cutter was used to cut the 1.1 mm circlip groove.

The part was then flipped in the lathe and the chuck changed to a collar chuck to prevent damaging the cut finish. The remaining length of the axle shaft required was measured and marked using callipers. Using a parting tool, the excess material was then cut, and the end faced off. An identical process was then used to make the required cuts on this right side.

The milling machine was then used to cut a flat on the shaft at the position of the grub screw.

5.2. Driveshaft

The process for manufacturing the driveshaft was much the same. Initially, a cylindrical steel shaft with a diameter of 16 mm was chosen and a 180 mm long part was cut off using a bandsaw.

The position of the shaft in the chuck was calibrated by first facing off the end of the shaft to set the Z axis to zero on the lathe and then setting the X axis to the measured diameter by touching the cutting tool onto the outer diameter of the shaft (while it was turning). The shaft was then cut down to the relevant diameters for the required lengths. The sharp corners were then chamfered by switching the cutting tool on the lathe to a chamfer tool. The chamfer tool was then switched out for the circlip tool to form the 1.1 mm wide groove. Finally, the shaft was cut to its required length of 136.0 mm.

To finish off the shaft, the milling machine was used to cut flats on the shaft at the three gear locations for each grub screw.

6. Conclusion

This project has seen us design and manufacture a four-wheel drive, two stage transmission car of length 230 mm, height 94 mm and width 80 mm. Though at the time of writing this report, the assembly of the car is not complete, its mass is estimated to be 1.8 kg, reasonably close to our target mass of 1.9 kg. Therefore, it will operate close to the planned output torque of 0.2125 Nm and speed 1.91 m/s. Our design also met our target of simplicity. Examples of this include the use of mid plates to provide structural rigidity as well as a means to mount components and constraining methods that constrain both axially and radially. Furthermore, using the driveshaft and bevel gears to achieve a two stage, four-wheel drive meant using less components than a full spur gear or belt and pulley transmission. A potential failure mode of our car is the possible fracturing of its plastic wheels, though a stress analysis of the wheels has been neglected in this report since they were given and could not be altered. Furthermore, as noted in Section 4.6, if all 80g of the test load were applied to only one axle shaft, its maximum stress would be very close to the yield stress (though this is an unlikely scenario where the load acts completely on either the front or back of the car's top surface). Overall, we are pleased with our execution of this project.

7. Inspection Report

Table 5 below shows an inspection report for an axle shaft and the driveshaft. The dimension IDs referred to in the table are labelled on the relevant engineering drawings at the end of this report.

Table 5: An inspection report recording measurements for an axle shaft and the driveshaft

Part number: EIF-11				
Description: AXLE SHAFT				
Dimension ID	Value and Tolerance	Measurement tool & method	Recorded measurement	Conclusion
AS1	0.00 11.5 -0.11	Micrometer	11.400	Met tolerance
AS2	+0.14 1.1 0.00	Callipers	1.21	Met tolerance
AS3	+0.05 8.00 0.00	Callipers	8.03	Met tolerance
AS4	90.0	Callipers	90.14	Met tolerance
AS5	11	Callipers	11.30	Met tolerance
AS6	+0.005 12 j5 -0.003	Micrometer	12.050	It is very difficult to reach this tolerance by hand, however this is adequate to fit the bearing.
AS7	18	Callipers	18.11	Met tolerance
AS8	33	Callipers	33.02	Met tolerance
AS9	126	Callipers	126.13	Met tolerance
AS10	18	Callipers	18.05	Met tolerance
AS11	0.0 31.0 -0.1	Callipers	30.90	Met tolerance
AS12	-0.1 14.0 -0.2	Micrometer	13.860	Met tolerance
AS13	R0.2			Too small to measure but the tool cuts a 0.2 radius fillet anyway
AS14	17.5	Callipers	17.5	Met tolerance
AS15	-0.006 14 q6 -0.017	Micrometer	14.030	It is very difficult to reach this tolerance by hand, however this is adequate to fit the bearing.
AS16	8.00	Micrometer	8.010	Met tolerance
AS17	18	Micrometer	18.050	Met tolerance
AS18	13.5	Micrometer	13.620	Met tolerance
AS19	Concentricity 0.01	Concentricity Gauge	0.02	Acceptable concentricity
AS20	Roughness Ra 1.2			
Part number: EIF-12				
Description: DRIVESHAFT				
Dimension ID	Value and Tolerance	Measurement tool & method	Recorded measurement	Conclusion
DS1	10	Callipers	10.20	Met tolerance
DS2	9	Callipers	10.04	Due to mistake at BS3
DS3	+0.1 23.0 0.0	Callipers	24.01	This was an error but it will not affect the design as it gives more room to position the gear.
DS4	+0.1 65.0 0.0	Callipers	65.20	Met tolerance
DS5	+0.1 136.0 0.0	Callipers	136.10	Met tolerance
DS6	6.00	Micrometers	6.010	Met tolerance
DS7	R0.2	N/A	N/A	Too small to measure but the tool cuts a 0.2 radius fillet
DS8	+0.1 25.4 0.0	Callipers	25.40	Met tolerance
DS9	9	Callipers	9.50	Met tolerance
DS10	+0.1 22.0 0.0	Callipers	22.05	Met tolerance
DS11	0.0 32.5 -0.1	Callipers	32.41	Met tolerance
DS12	14	Micrometers	14.100	Met tolerance
DS13	9.5	Micrometers	9.620	Met tolerance
DS14	+0.005 12 j5 -0.003	Micrometers	12.010	It is very difficult to reach this tolerance by hand, however this is adequate to fit the bearing.
DS15	-0.005 10 q6 -0.014	Micrometers	10.020	It is very difficult to reach this tolerance by hand, however this is adequate to fit the bearing.
DS16	20	Callipers	20.11	Met tolerance
DS17	11.5	Micrometers	11.450	Met tolerance
DS18	-0.005 12 q6 -0.014	Micrometers	12.040	It is very difficult to reach this tolerance by hand, however this is adequate to fit the bearing.
DS19	+0.005 12 j5 -0.003	Micrometers	12.030	Met tolerance
DS20	+0.14 1.10 0.00	Callipers	1.15	Met tolerance
DS21	0.00 11.50 -0.11	Micrometers	11.430	Met tolerance
DS22	Concentricity 0.01	Concentricity Gauge	0.01	Acceptable Concentricity
DS23	Roughness Ra 1.2			

8. Appendices

A1 – Shear Stress on the Motor Shaft

The force acting on the inner surface of the keyless bush was calculated from the shear force of the torque. Dividing this by the area of the inner surface of the keyless bush over which the shear force acts, we obtained the following equation for the shear stress:

$$\tau = \frac{\left(\frac{T}{r}\right)}{2\pi r l} = \frac{\left(\frac{0.085}{0.0025}\right)}{2\pi \times 0.0025 \times 0.00625} = 346321 \text{ Pa} \quad (9)$$

A2 – Grub Screw Torsional Holding Capacity (THC)

Equation 10 below is true for constraining of shaft elements. Looking up the quoted value of the axial holding capacity (AHC) for an M4 size grub screw on a mild steel shaft, we found this to be 163 N (*safetysocket.com*). Multiplying this by the radius of the relevant part of the axle shaft, the shaft that experiences the maximum torque in the system, we obtain:

$$AHC \times \text{Shaft Radius} = THC = 163 \times 0.014 = 2.282 \text{ Nm} \quad (10)$$

B1 – Free Body Diagram Calculations

During motion, the friction force is given by the product of the dynamic coefficient of friction and the normal reaction force. Furthermore, due to the car having a fairly uniform distribution of mass and being supported by only the four wheels, we can say that the reaction force on a single wheel is simply the weight of the car divided by four. Therefore, the following statements could be made:

$$f = \mu_d R \quad R = W = \frac{mg}{4} \quad F = \mu_d \frac{mg}{4} \quad (11)$$

We can relate this to total output torque T_O by multiplying F by wheel radius r and then multiplying this by four to take into account all four wheel. Where wheel radius r was 32.5 mm, dynamic coefficient of friction of the concourse's granite floor was approximated to be 0.35 and the mass of the car was approximated to end up being 2 kg, we obtained:

$$T_O = 4 \times F \times r = \mu_d r m g = 0.35 \times 0.0325 \times 2 \times 9.81 = 0.223 \text{ Nm} \quad (12)$$

B2 – Gear Ratio Calculations

From the motor specification sheet provided, it could be seen that to achieve maximum motor power we would need the motor shaft to operate at 0.085 Nm (which would correspond to an angular velocity of 1400 rpm). As demonstrated above, the torque output when a mass of 2kg was presumed was 0.223 Nm. Therefore, the overall torque amplification required to operate at maximum power was:

$$R = R_1 \times R_2 = \frac{T_{axles}}{T_{motor}} = \frac{0.223}{0.085} = 2.62 \quad (13)$$

Where R_1 and R_2 are the first and second stage drive ratios. Various PCD combinations were tried until this ratio was approximately attained by using the PCDs in Table 6. The selection of gears was limited by the spatial constraints of the overall design. The selected gears have a gear module of 1.5 mm.

Table 6 – Pitch Circle Diameter of the selected gears

Gear	Motor Shaft Spur	Driveshaft Spur	Driveshaft Bevels	Axle Shaft Bevels
PCD	36 mm	45 mm	22.5 mm	45 mm

As demonstrated, this achieved a torque amplification of 2.5 (slightly less than our initial target ratio).

$$R_{actual} = R_1 \times R_2 = \frac{PCD_{driveshaft-spur}}{PCD_{motor-spur}} = \frac{PCD_{axle-bevel}}{PCD_{driveshaft-bev}} = \frac{45}{36} \times \frac{45}{22.5} = 2.5 \quad (14)$$

Therefore, in order to still achieve maximum power with this drive ratio, our target mass had to be adjusted to 1.9 kg as shown.

$$T_O = R_{actual} \times T_{motor} = 2.5 \times 0.085 = 0.2125 \text{ Nm} \quad (15)$$

$$m_{target} = \frac{T_o}{\mu_d \times r \times g} = \frac{0.2125}{0.35 \times 0.0325 \times 9.81} = 1.90 \text{ kg} \quad (16)$$

Since power could be taken as constant throughout the system due to high efficiency of gears, the output torque could be related to its speed so that the car's speed could be calculated, and its suitability confirmed.

$$P = P_{motor} = T_{motor} \times \omega_{motor} = 0.085 \times 1400 \times \frac{2\pi}{60} = 12.46 \text{ W} \quad (17)$$

$$\omega_{axle} = \frac{P}{T_{axle}} = \frac{12.46}{0.2125} = 58.64 \text{ rad/s} \quad (18)$$

$$V_{car} = \omega_{axle} \times r_{whe} = 58.64 \times 0.0325 = 1.91 \text{ m/s} \quad (19)$$

C1 – Lewis Equation Calculations

The minimum required face width, w_{min} , of our gears was calculated using the Lewis Equation (examining only pinion gears as they are subject to higher loads):

$$w = \frac{F \times 10^6}{K \times m \times Y \times \sigma_p} \quad (20)$$

Taking the spur gears as an example, F was calculated by dividing the relevant shaft power by the radial velocity of the gear:

$$F_{spur} = \frac{P}{v} = \frac{T_{motor} \times \omega_{motor}}{r_{spur} \times \omega_{spur}} = \frac{0.085 \times 146.6}{0.018 \times 146.6} = 4.72 \text{ N} \quad (21)$$

The velocity factor K was calculated from the Barth equation:

$$K_{spur} = \frac{6.1}{6.1 + v} = \frac{6.1}{6.1 + r_{spur} \times \omega_{spur}} = \frac{6.1}{6.1 + 0.018 \times 146.6} = 0.70 \quad (22)$$

This, combined with the maximum permissible material stress of 42 MPa, a Y constant of 0.33056 (Gosling, 2018), and the gear module m of 1.5 gave a minimum required face width of 0.325 mm. The process was repeated for the bevel gears giving a minimum required face width of 0.685 mm. Both were much less than the face widths of our chosen gears (12 mm for spur and 7.55 mm for bevel).

C2 – Bearing Calculations

Firstly, the minimum L_{10} bearing life was calculated by finding the number of revolutions of the wheel per second (using the target velocity, v_{target} and the wheel diameter, D_{wheel}) and multiplying this by the number of seconds in a 100-hour service life (since this was the specified service life requirement):

$$L_{10} = \frac{v_{target}}{\pi \times D_{wheel}} \times 360,000 \text{ sec} = \frac{2.1}{\pi \times 0.065} \times 360,000 \text{ sec} = 4.4 \times 10^6 \text{ revs} \quad (23)$$

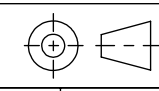
Now, considering the worst-case scenario of only one shaft taking the maximum load of 80 kg, the radial load F_r on a single bearing was calculated to be half of that load at $F_r = 392.4 \text{ N}$. Since there was assumed to be no axial forces present, the total maximum load on a single bearing was the maximum radial force, F_r .

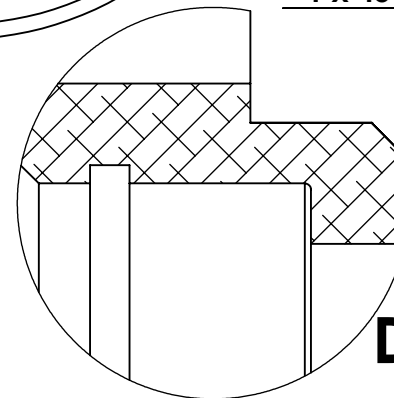
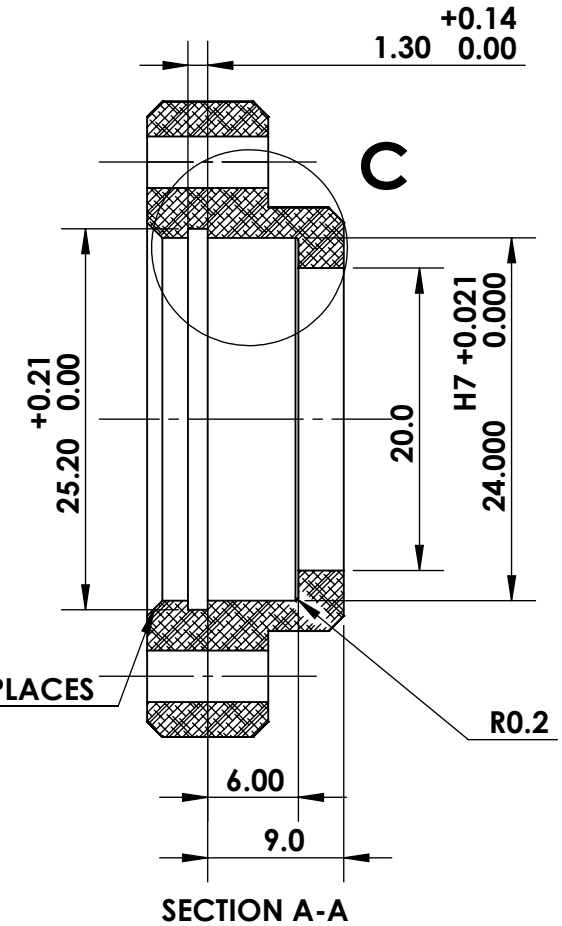
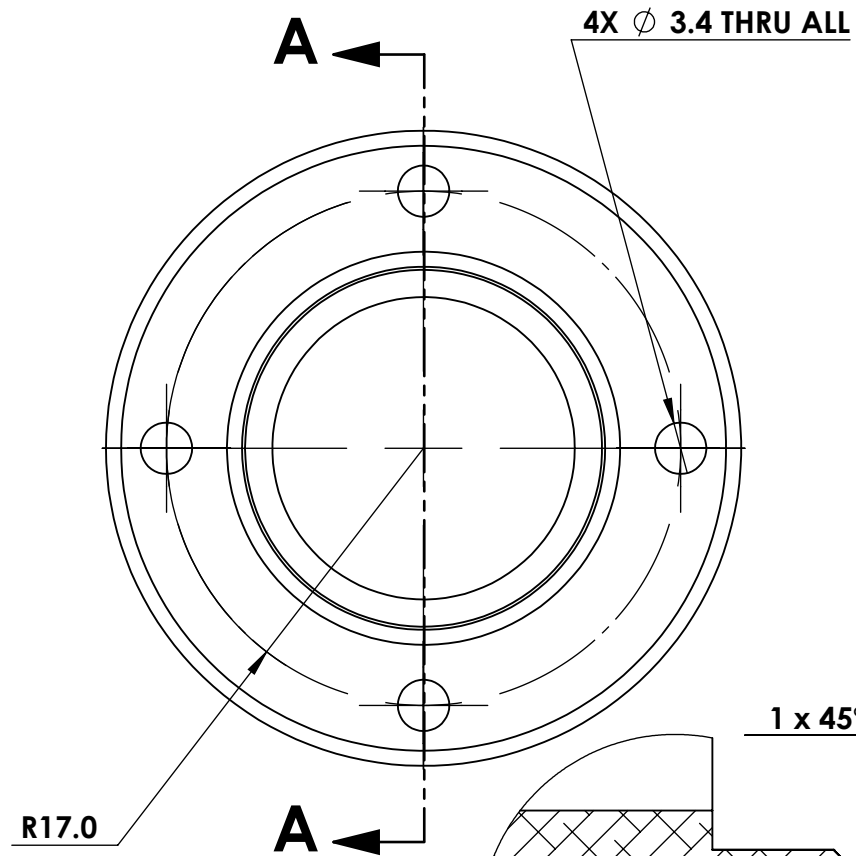
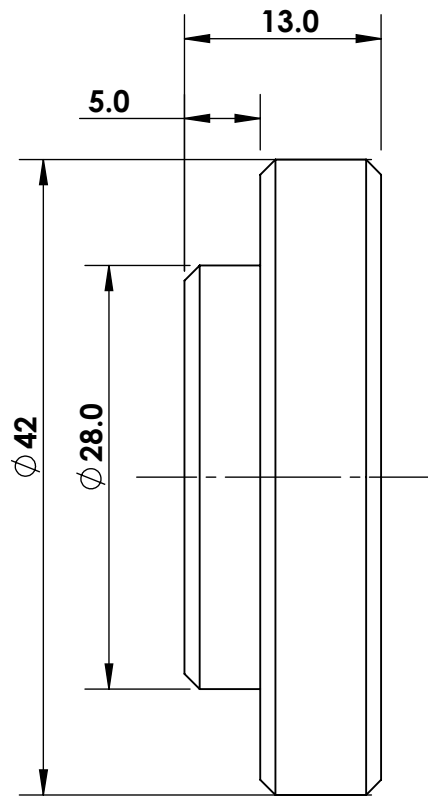
The minimum dynamic load rating, C_{min} , that the bearing will require to withstand the 80g force and run for 100 hours was found using the equation below:

$$C_{min} = F_r \cdot (L_{10})^{1/k} \quad (24)$$

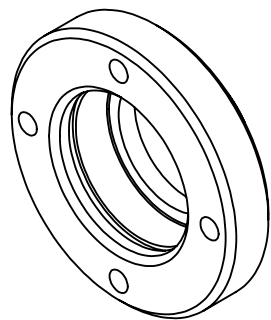
Using a k value of 3, the quoted value for a ball bearing (Gosling, 2017), the minimum dynamic load was $C_{min} = 659.43 \text{ N}$. This meant the SKF bearing 61901 with a dynamic load rating $C = 2.91 \text{ kN}$ was well above the required C_{min} value and so was used throughout our whole design.

ITEM NO.	PART NUMBER	DESCRIPTION	QTY.	MATERIAL	EXTRA NOTES
1	EIF-3-GP-24	MIDPLATE BACK	1	ALUMINIUM 6082 T6	
2	EIF-15-GP-24	MOTOR	1	VARIOUS	PROVIDED BY THE MECHANICAL ENGINEERING DEPARTMENT
3	EIF-5-GP-24	MIDPLATE FRONT	1	ALUMINIUM 6082 T6	
4	EIF-4-GP-24	MIDPLATE	1	ALUMINIUM 6082 T6	
5	EIF-17-GP-24	WHEEL HUB	4	PLASTIC	PROVIDED BY THE MECHANICAL ENGINEERING DEPARTMENT (BUT MODIFIED)
6	EIF-18-GP-24	TYRE	4	RUBBER	PROVIDED BY THE MECHANICAL ENGINEERING DEPARTMENT
7	EIF-11-GP-24	AXLE SHAFT	2	MILD STEEL EN1A	
8	EIF-19-GP-24	KEYLESS BUSH - 5mm ID - RS 778-4935	1	VARIOUS	
9	EIF-1-GP-24	24MM ID BEARING HOUSING	5	ALUMINIUM 6082 T6	
10	EIF-20-GP-24	INTERNAL CIRCLIP - B024M	6	CARBON STEEL	FROM STUDENT TEACHING WORKSHOP
11	EIF-21-GP-24	SKF BALL BEARING - 61901 - RS 144-0862	6	VARIOUS	
12	EIF-13-GP-24	SIDE PLATE	2	ALUMINIUM 6082 T6	
13	EIF-22-GP-24	SOCKET HEAD SCREW - M3 X 12	32	CARBON STEEL	FROM STUDENT TEACHING WORKSHOP
14	EIF-6-GP-24	HACKSAWED 24MM ID BEARING HOUSING	1	ALUMINIUM 6082 T6	SAME AS EIF-1-GP-24 BUT THE TOP IS HACKSAWED
15	EIF-23-GP-24	EXTERNAL CIRCLIP - S012M	3	CARBON STEEL	FROM STUDENT TEACHING WORKSHOP
16	EIF-24-GP-24	M3 HEX FULL NUT	55	STAINLESS STEEL	FROM STUDENT TEACHING WORKSHOP
17	EIF-25-GP-24	BATTERY PACK	1	VARIOUS	PROVIDED BY THE MECHANICAL ENGINEERING DEPARTMENT
18	EIF-26-GP-24	SOCKET HEAD SCREW - M3 X 16	23	CARBON STEEL	FROM STUDENT TEACHING WORKSHOP
19	EIF-12-GP-24	DRIVESHAFT	1	MILD STEEL EN1A	
20	EIF-8-GP-24	PLASTIC BEVEL GEAR - HPC ZBD1.5-30	2	DELRIN	
21	EIF-7-GP-24	PLASTIC BEVEL PINION GEAR - HPC ZBD1.5-15	2	DELRIN	
22	EIF-27-GP-24	GRUB SCREW - M4 X 6	5	CARBON STEEL	FROM STUDENT TEACHING WORKSHOP
23	EIF-10-GP-24	PLASTIC SPUR GEAR - HPC ZG1.5-30	1	DELRIN	
24	EIF-9-GP-24	PLASTIC SPUR PINION GEAR - HPC ZG1.5-24	1	DELRIN	
25	EIF-16-GP-24	PLASTIC COVER	1	ABS	
26	EIF-2-GP-24	L-PLATE	8	ALUMINIUM 6082 T6	
27	EIF-28-GP-24	FRONT GUIDE BUMPER	1	ALUMINIUM 6082 T6	
28	EIF-29-GP-24	BACK GUIDE BUMPER	1	ALUMINIUM 6082 T6	
29	EIF-32-GP-24	COUNTERSUNK FLAT SCREW - M4 X 6	4	CARBON STEEL	FROM STUDENT TEACHING WORKSHOP

TOLERANCES X = ± 0.5 X.X = ± 0.1 X.XX = ± 0.02		THIRD ANGLE PROJECTION 		MATERIAL: N/A ALL DIMENSIONS ARE IN MILLIMETRES		TITLE: BOM - Long form		Imperial College London Department of Mechanical Engineering	
NAME DRAWN SYED AHAMED CHECKED ASAD RAJA APPROVED ASAD RAJA		DATE 02.12.18 03.12.18 03.12.18		DO NOT SCALE DRAWING A3 SCALE N/A		DWG No. EIF-33-GP-24		SHEET 1 OF 1 REVISION 0	



DETAIL C
SCALE 4 : 1



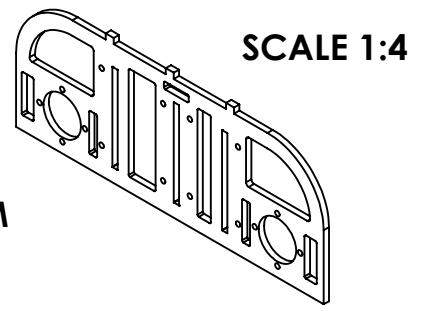
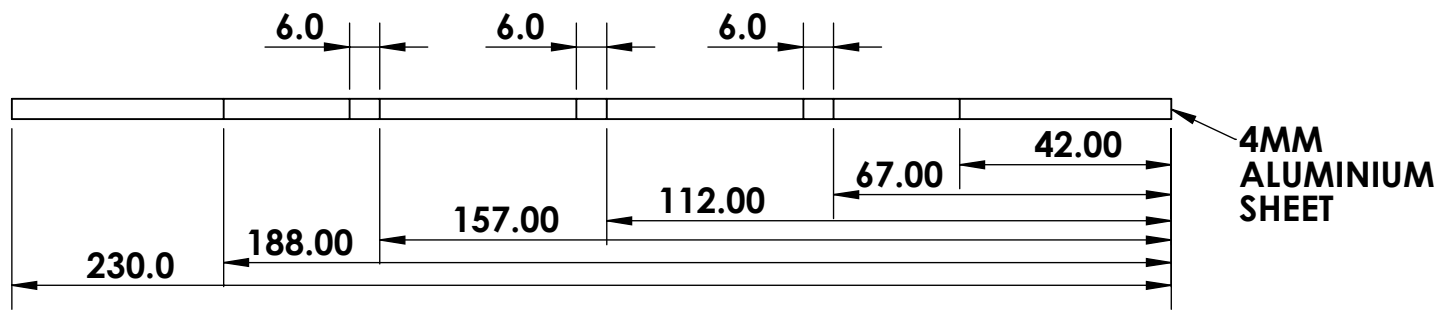
Scale: 1:1

TOLERANCES		THIRD ANGLE PROJECTION	
X	± 0.5	ANGULAR	± 1°
X.X	± 0.1	SURFACE FINISH	MACHINED
X.XX	± 0.02	FACES	Ra 6.3
	NAME	DATE	
DRAWN	FARHADUL ISLAM	28.10.18	
CHECKED	WENBO CHEN	08.11.18	
APPROVED	RAJIV SAMANTA	09.11.18	

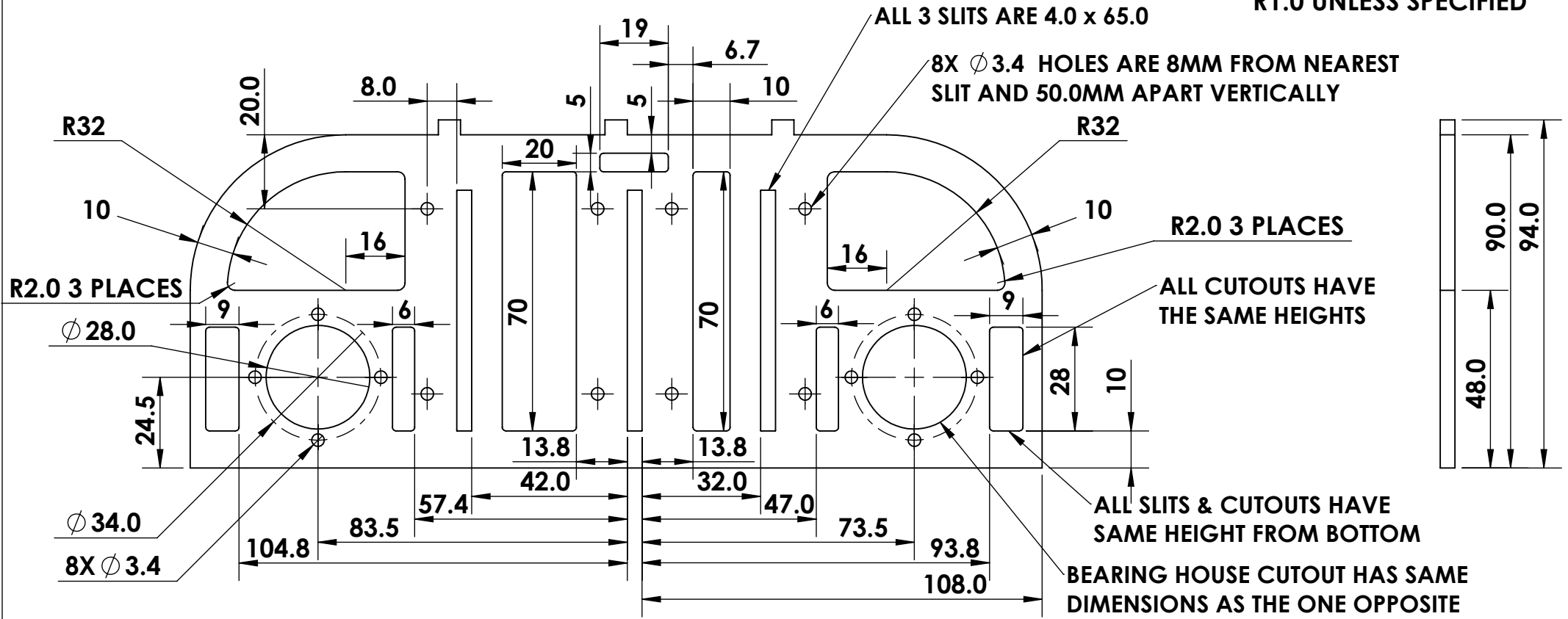
MATERIAL: ALUMINIUM 6082 T6	
ALL DIMENSIONS ARE IN MILLIMETRES	
DO NOT SCALE DRAWING	
A4	SCALE 2:1

TITLE: BEARING HOUSING
DWG No. EIF-1-GP-24

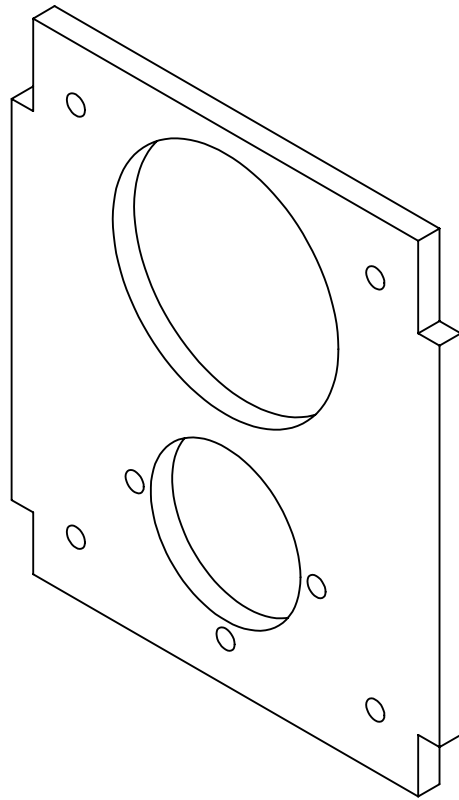
Imperial College London	
Department of Mechanical Engineering	
SHEET 1 OF 1	REVISION 1



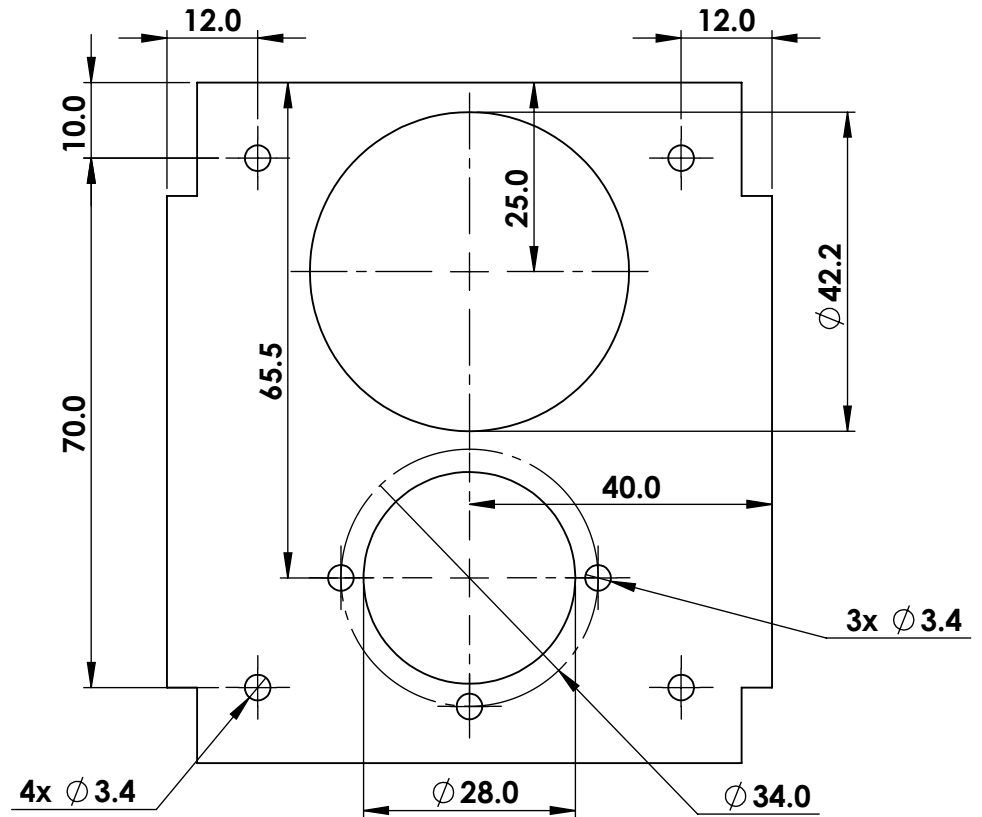
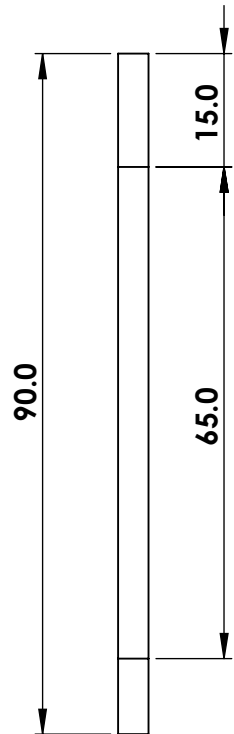
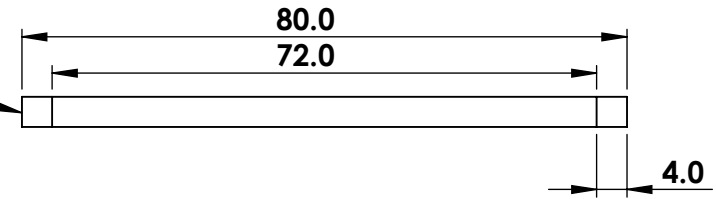
ALL CUTOUT FILLETS ARE R1.0 UNLESS SPECIFIED



TOLERANCES		THIRD ANGLE PROJECTION		MATERIAL: ALUMINIUM 6082 T6		TITLE: SIDE PLATE		Imperial College London Department of Mechanical Engineering					
X	= ± 0.5	ANGULAR ±1°		ALL DIMENSIONS ARE IN MILLIMETRES		DO NOT SCALE DRAWING				DWG No. EIF-13-GP-24			
X.X	= ± 0.1	SURFACE FINISH MACHINED						DRAWN				FARHADUL ISLAM	
X.XX	= ± 0.02	FACES Ra 6.3		DO NOT SCALE DRAWING		CHECKED		WENBO CHEN		02.11.18			
				A4		SCALE 2:3		APPROVED		RAJIV SAMANTA		02.11.18	
								SHEET 1 OF 1		REVISION 2			



LASER CUT 4mm PLATE

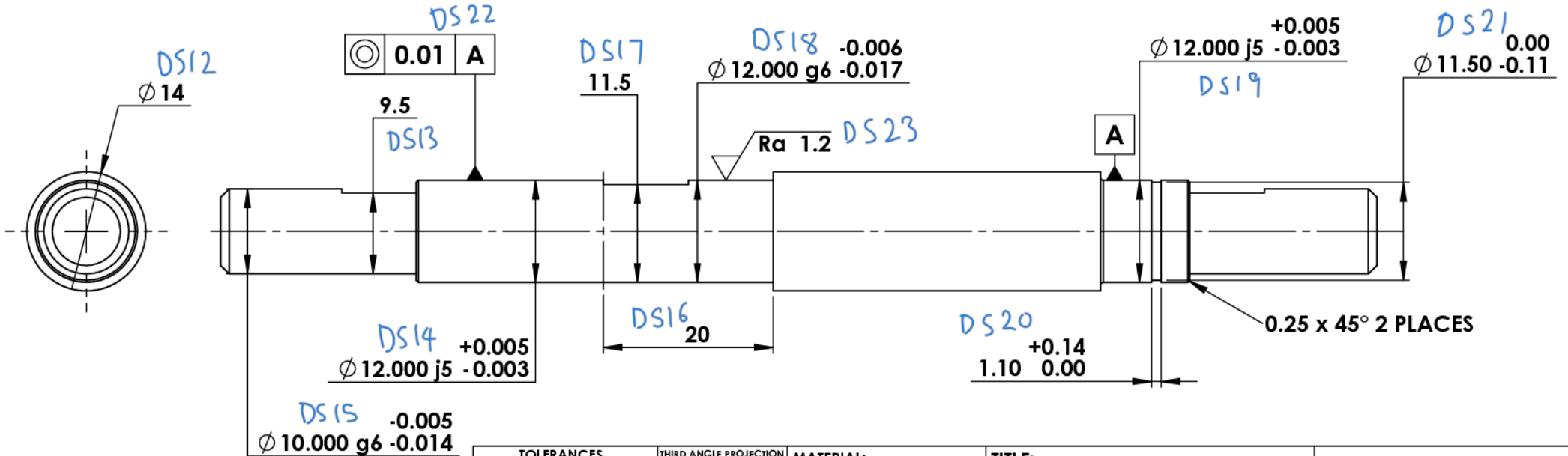
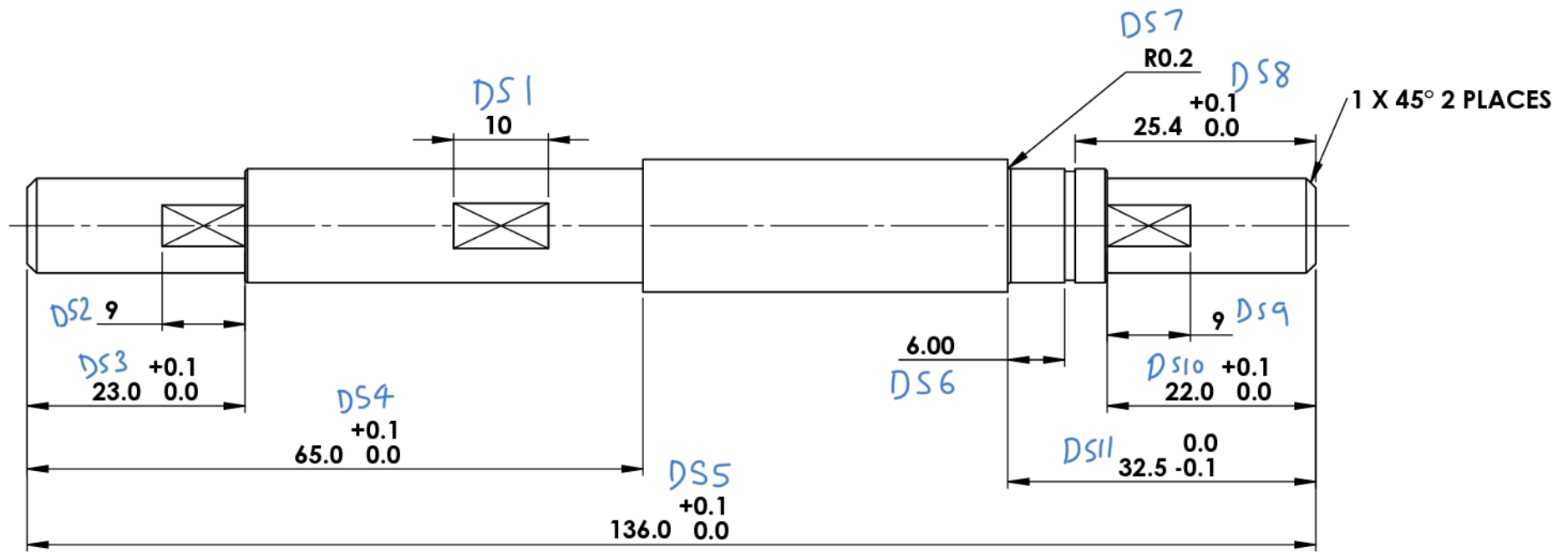


TOLERANCES		THIRD ANGLE PROJECTION	
X	± 0.5	ANGULAR	± 1°
X.X	± 0.1	SURFACE FINISH	MACHINED
X.XX	± 0.02	FACES	Ra 6.3
	NAME	DATE	
DRAWN	RAJIV SAMANTA	31.10.18	
CHECKED	FARHADUL ISLAM	01.11.18	
APPROVED	WENBO CHEN	02.11.18	

MATERIAL: ALUMINIUM 6082 T6	
ALL DIMENSIONS ARE IN MILLIMETRES	
DO NOT SCALE DRAWING	
A4	SCALE 1:1

TITLE: MIDPLATE BACK
DWG No. EIF-3-GP-24

Imperial College London	
Department of Mechanical Engineering	
SHEET 1 OF 1	REVISION 1



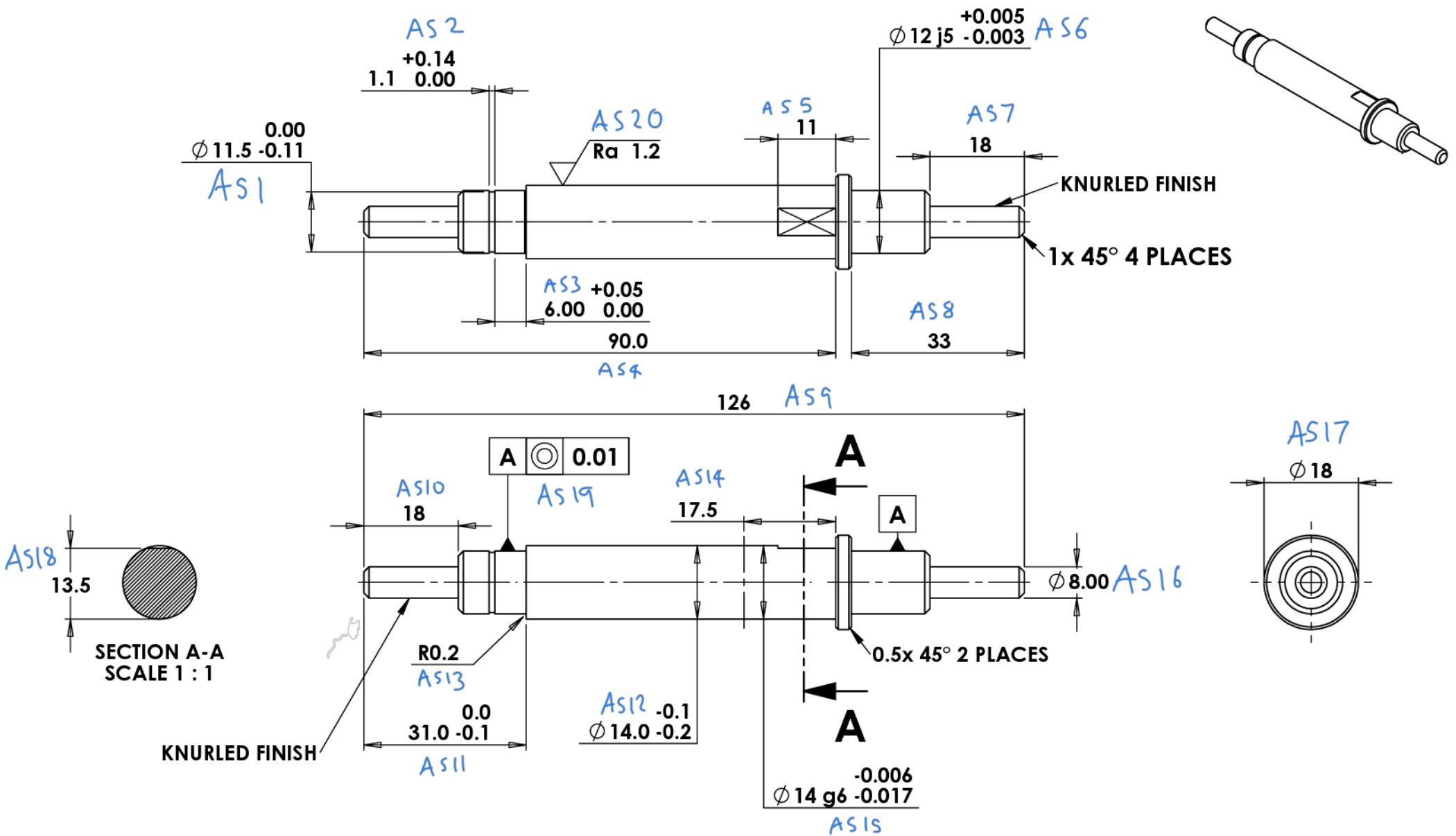
**INSPECTION REPORT
DIMENSION IDs SHOWN**

TOLERANCES		THIRD ANGLE PROJECTION	
X	± 0.5	ANGULAR	± 1°
X.X	± 0.1	SURFACE FINISH	MACHINED
X.XX	± 0.02	FACES	Ra 6.3
		NAME	DATE
DRAWN	ASAD RAJA	31.10.18	
CHECKED	WENBO CHEN	05.11.18	
APPROVED	RAJIV SAMANTA	10.11.18	

MATERIAL: MILD STEEL EN1A	
ALL DIMENSIONS ARE IN MILLIMETRES	
DO NOT SCALE DRAWING	
A4	SCALE 3:2

TITLE: DRIVESHAFT
DWG No. EIF-12-GP-24

Imperial College London	
Department of Mechanical Engineering	
SHEET 1 OF 1	REVISION 1



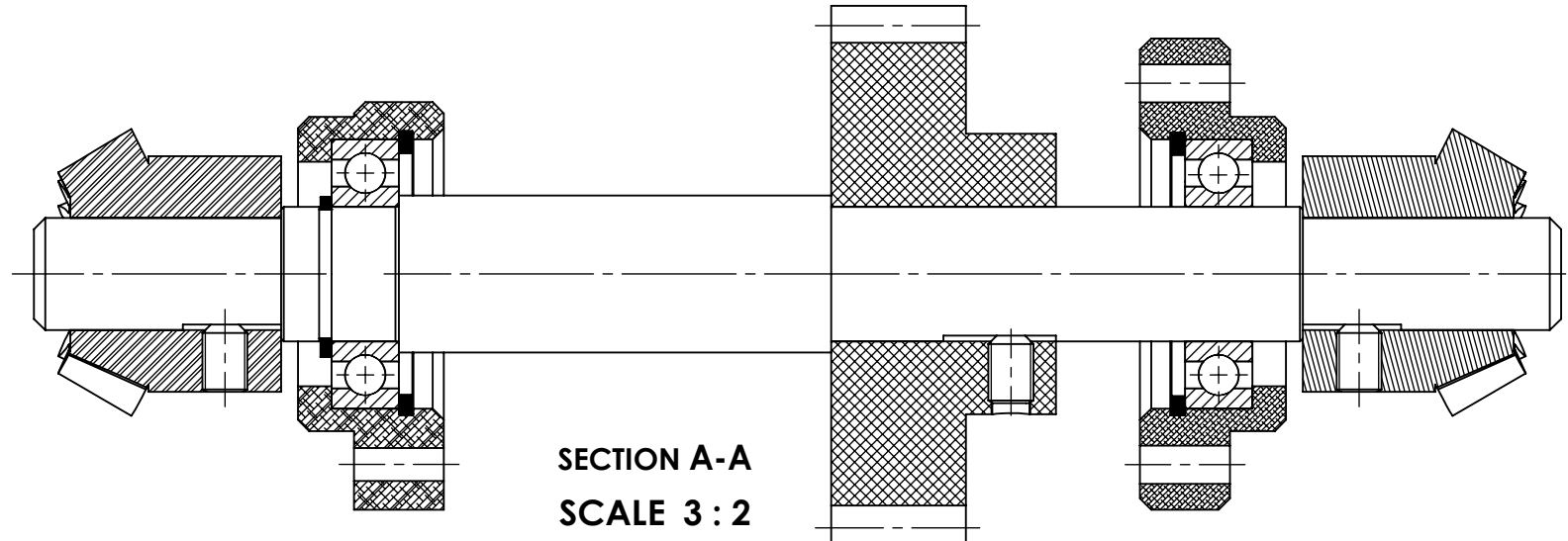
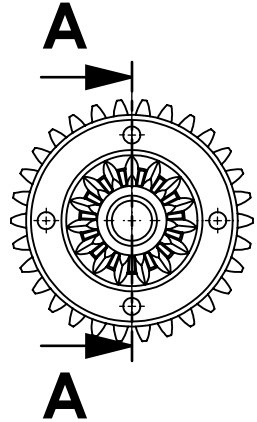
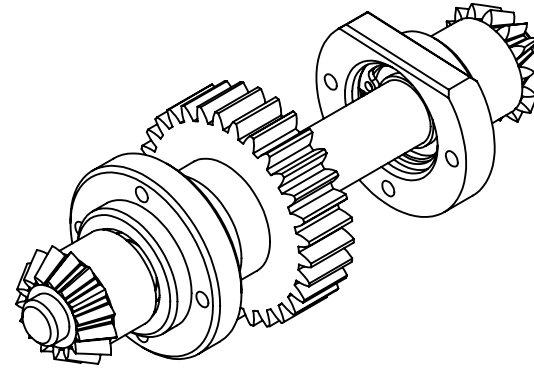
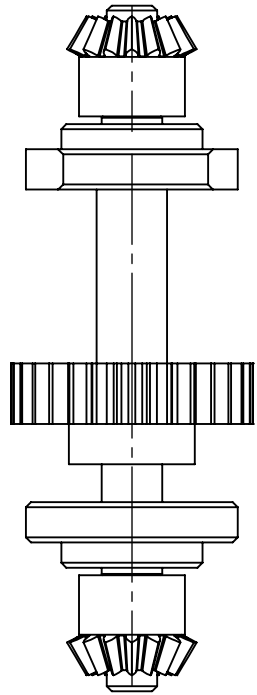
INSPECTION REPORT
DIMENSION IDs SHOWN

TOLERANCES		THIRD ANGLE PROJECTION	
X	± 0.5	ANGULAR	± 1°
X.X	± 0.1	SURFACE FINISH	MACHINED
X.XX	± 0.02	FACES	Ra 6.3
		NAME	DATE
DRAWN	ASAD RAJA	30.10.18	
CHECKED	RAJIV SAMANTA	31.10.18	
APPROVED	SYED AHAMED	04.11.18	

MATERIAL: MILD STEEL EN1 A	
ALL DIMENSIONS ARE IN MILLIMETRES	
DO NOT SCALE DRAWING	
A4	SCALE 1:1

TITLE: AXLE SHAFT
DWG No. EIF-11-GP-24

Imperial College London	
Department of Mechanical Engineering	
SHEET 1 OF 1	REVISION 1

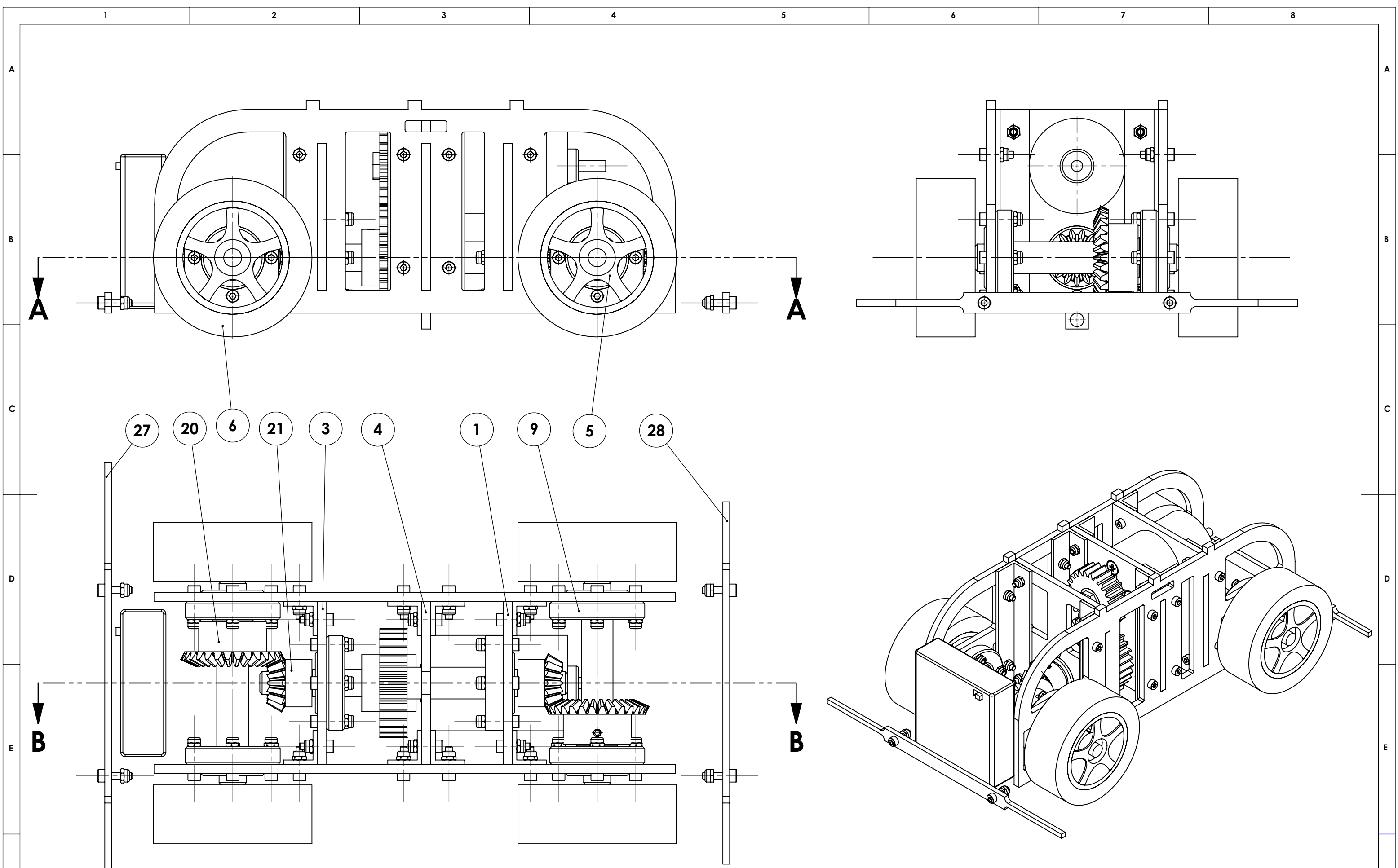


TOLERANCES		THIRD ANGLE PROJECTION	
X	± 0.5	ANGULAR	$\pm 1^\circ$
X.X	± 0.1	SURFACE FINISH	MACHINED
X.XX	± 0.02	FACES	Ra 6.3
	NAME	DATE	
DRAWN	ASAD RAJA	31.10.18	
CHECKED	FARHADUL ISLAM	02.11.18	
APPROVED	WENBO CHEN	06.11.18	

MATERIAL: VARIOUS	
ALL DIMENSIONS ARE IN MILLIMETRES	
DO NOT SCALE DRAWING	
A4	SCALE 2:3

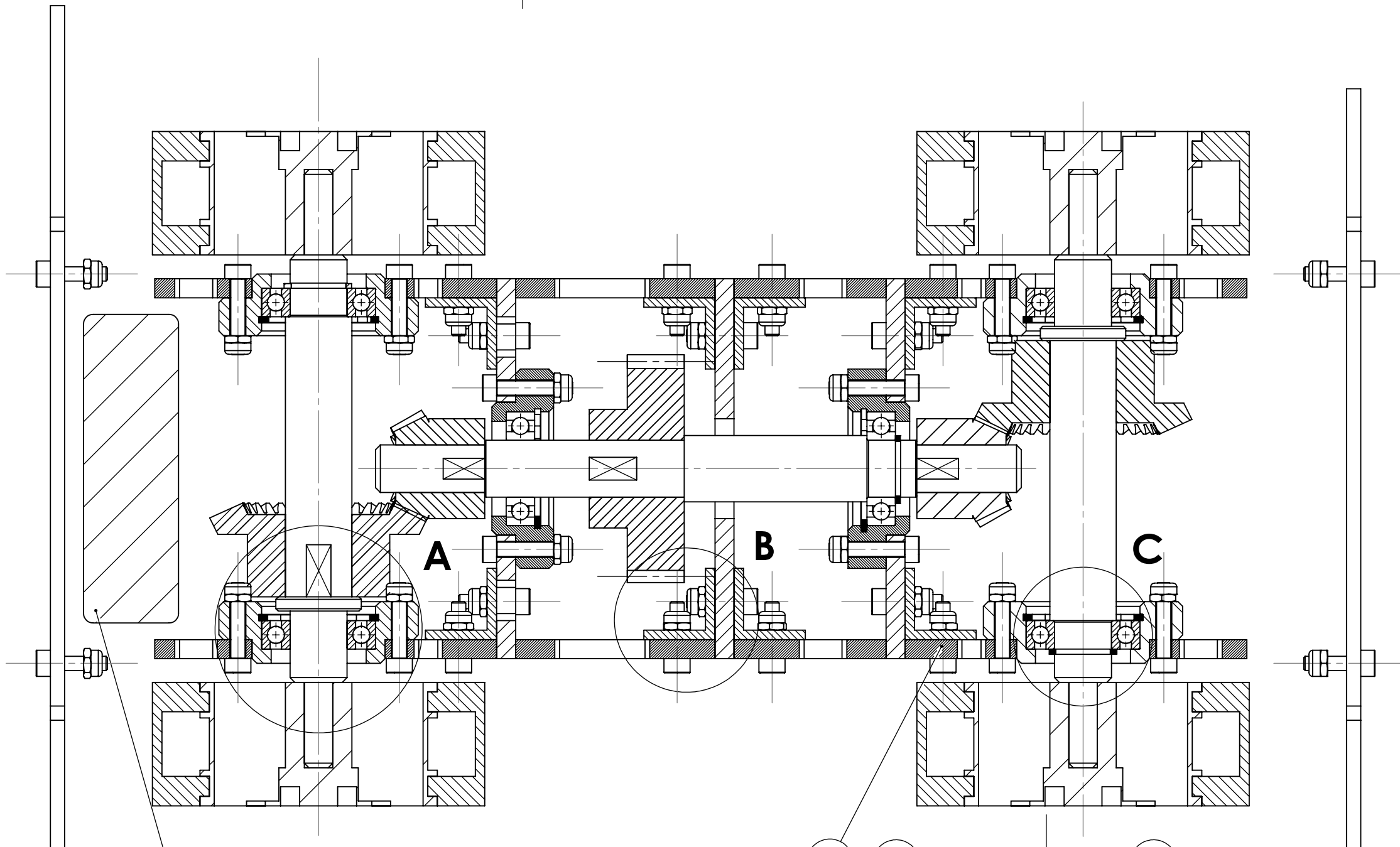
TITLE: DRIVESHAFT SUBASSEMBLY
DWG No. EIF-30-GP-24

Imperial College London	
Department of Mechanical Engineering	
SHEET 1 OF 1	REVISION 1

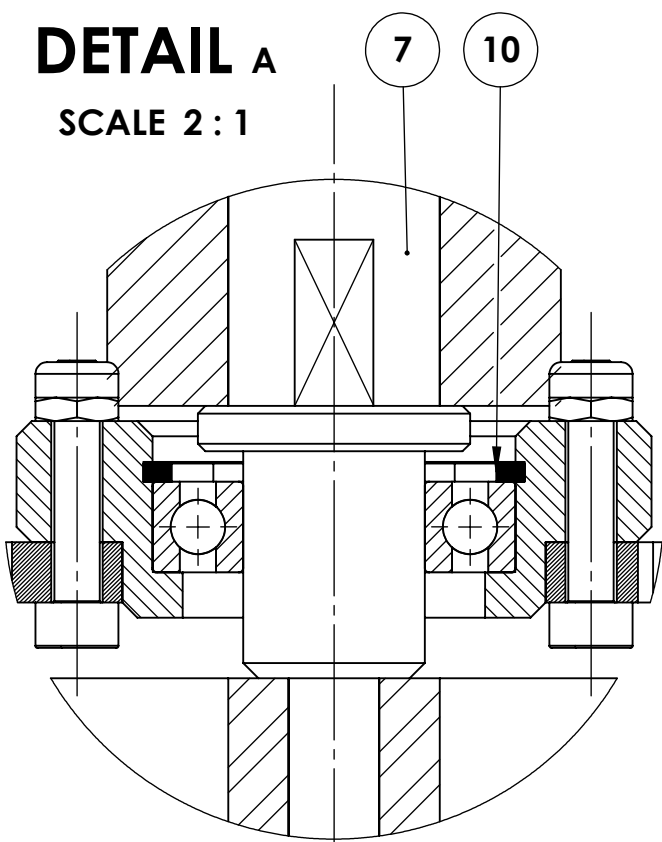


TOLERANCES X = ± 0.5 X.X = ± 0.1 X.XX = ± 0.02		THIRD ANGLE PROJECTION 		MATERIAL: VARIOUS ALL DIMENSIONS ARE IN MILLIMETRES		TITLE: FULL ASSEMBLY		Imperial College London Department of Mechanical Engineering	
				DO NOT SCALE DRAWING		DWG No. EIF-31-GP-24		SHEET 1 OF 4 REVISION 1	
				A3 SCALE 2:3					

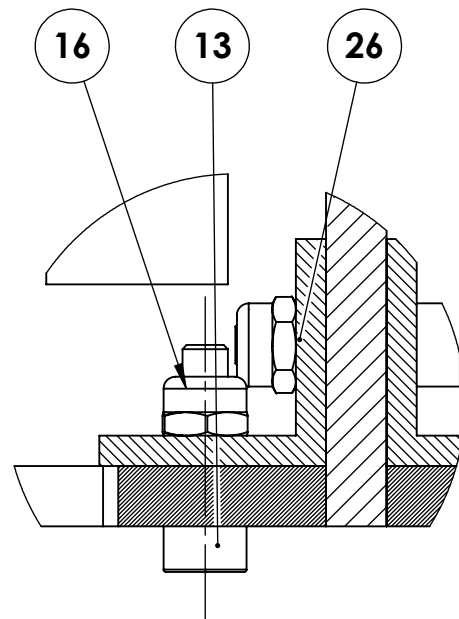
SECTION A-A



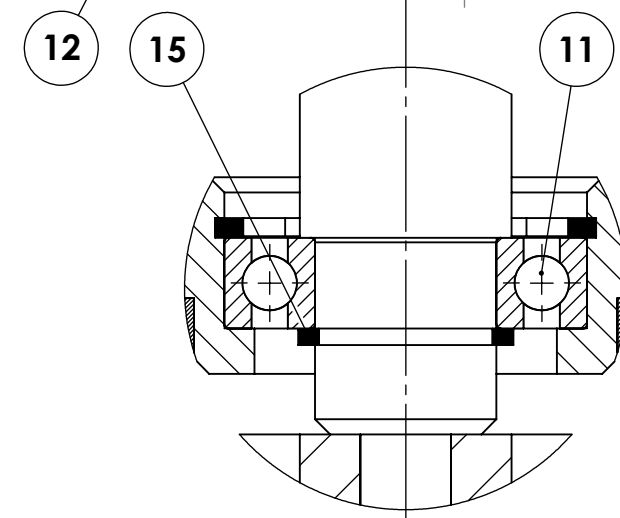
DETAIL A
SCALE 2:1



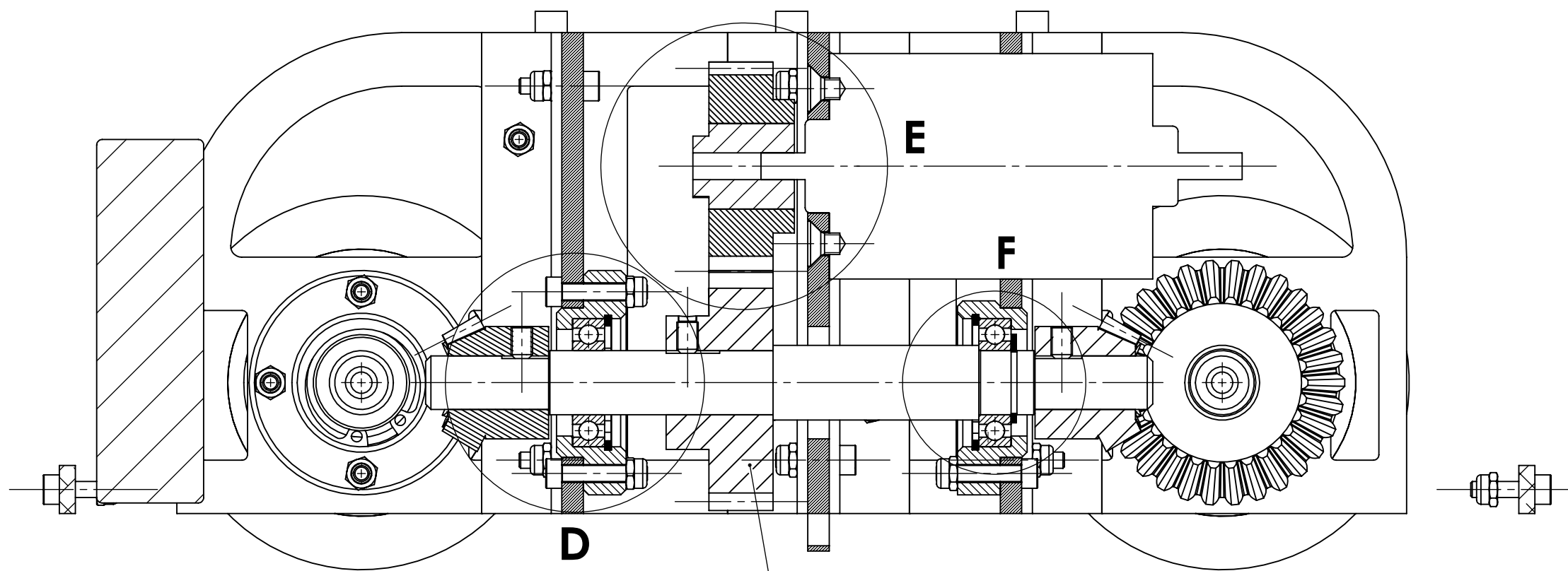
DETAIL B
SCALE 2:1



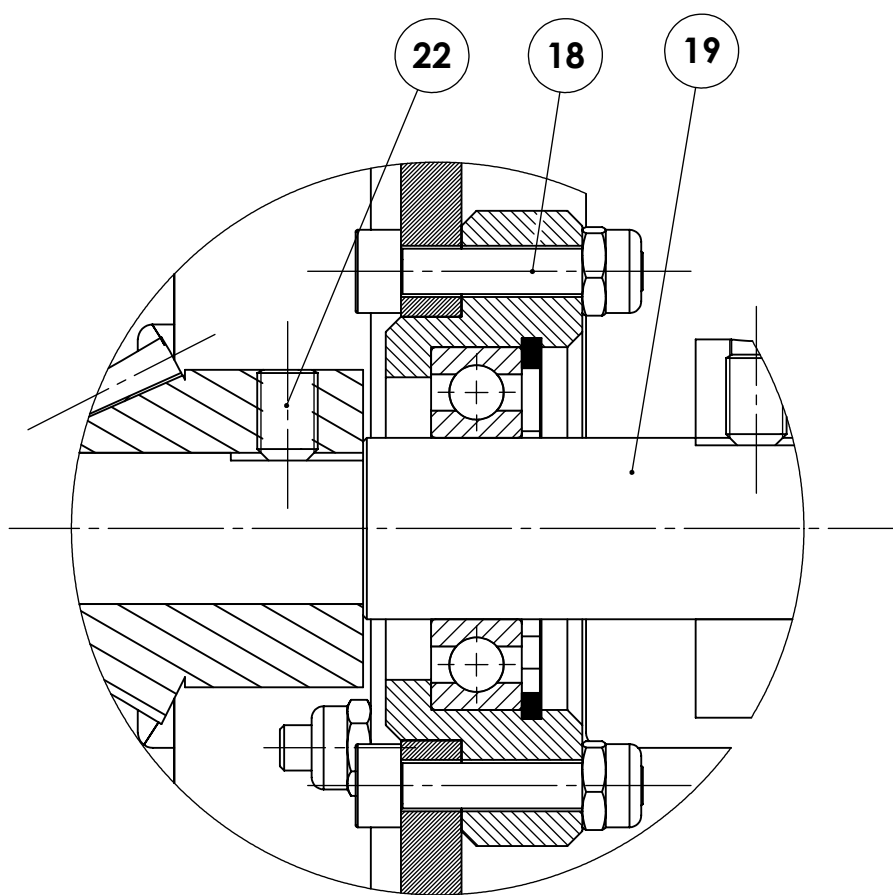
DETAIL C
SCALE 2:1



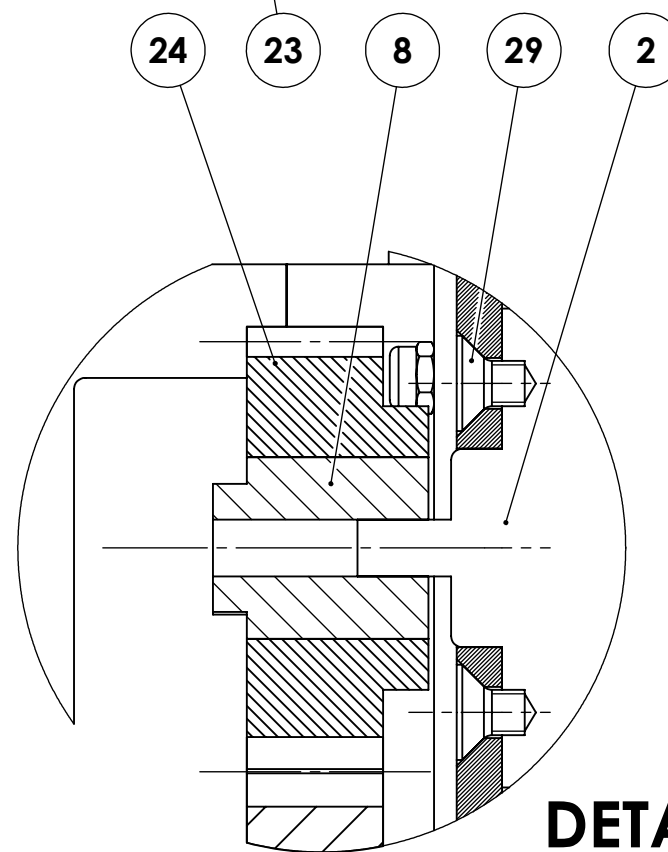
TOLERANCES X = ± 0.5 X.X = ± 0.1 X.XX = ± 0.02		THIRD ANGLE PROJECTION 		MATERIAL: VARIOUS		TITLE: FULL ASSEMBLY		Imperial College London Department of Mechanical Engineering	
ANGULAR ±1° SURFACE FINISH MACHINED FACES Ra 6.3		DO NOT SCALE DRAWING		ALL DIMENSIONS ARE IN MILLIMETRES		DWG No. EIF-31-GP-24		SHEET 2 OF 4 REVISION 1	
NAME FARHADUL ISLAM		DATE 01.11.18		A3		SCALE 1:1			
DRAWN FARHADUL ISLAM		CHECKED WENBO CHEN		APPROVED RAJIV SAMANTA					



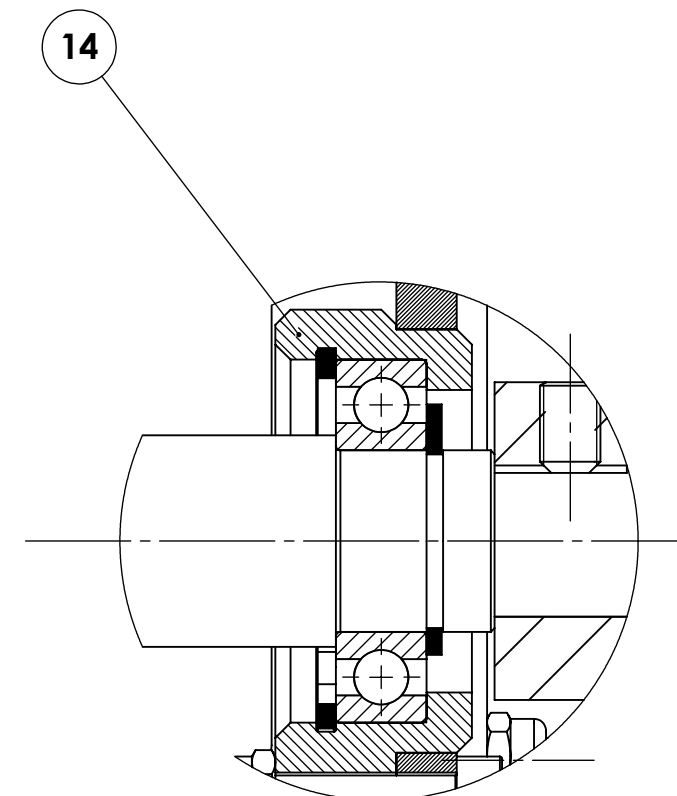
SECTION B-B



DETAIL D
SCALE 2 : 1



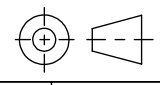
DETAIL E
SCALE 3 : 2



DETAIL F
SCALE 2 : 1

TOLERANCES X = ± 0.5 X.X = ± 0.1 X.XX = ± 0.02		THIRD ANGLE PROJECTION 	MATERIAL: VARIOUS ALL DIMENSIONS ARE IN MILLIMETRES	TITLE: FULL ASSEMBLY	Imperial College London Department of Mechanical Engineering
NAME FARHADUL ISLAM		DATE 01.11.18	DO NOT SCALE DRAWING A3 SCALE 1:1	DWG No. EIF-31-GP-24	
DATE 04.11.18		DATE 05.11.18	SHEET 3 OF 4 REVISION 1		

ITEM NO.	PART NUMBER	DESCRIPTION	QTY.
1	EIF-3-GP-24	MIDPLATE BACK	1
2	EIF-15-GP-24	MOTOR	1
3	EIF-5-GP-24	MIDPLATE FRONT	1
4	EIF-4-GP-24	MIDPLATE	1
5	EIF-17-GP-24	WHEEL HUB	4
6	EIF-18-GP-24	TYRE	4
7	EIF-11-GP-24	AXLE SHAFT	2
8	EIF-19-GP-24	KEYLESS BUSH - 5mm ID - RS 778-4935	1
9	EIF-1-GP-24	24MM ID BEARING HOUSING	5
10	EIF-20-GP-24	INTERNAL CIRCLIP - B024M	6
11	EIF-21-GP-24	SKF BALL BEARING - 61901 - RS 144-0862	6
12	EIF-13-GP-24	SIDE PLATE	2
13	EIF-22-GP-24	SOCKET HEAD SCREW - M3 X 12	32
14	EIF-6-GP-24	HACKSAWED 24MM ID BEARING HOUSING	1
15	EIF-23-GP-24	EXTERNAL CIRCLIP - S012M	3
16	EIF-24-GP-24	M3 NUT	55
17	EIF-25-GP-24	BATTERY PACK	1
18	EIF-26-GP-24	SOCKET HEAD SCREW - M3 X 16	23
19	EIF-12-GP-24	DRIVESHAFT	1
20	EIF-8-GP-24	PLASTIC BEVEL GEAR - HPC ZBD1.5-30	2
21	EIF-7-GP-24	PLASTIC BEVEL PINION GEAR - HPC ZBD1.5-15	2
22	EIF-27-GP-24	GRUB SCREW - M4 X 6	5
23	EIF-10-GP-24	PLASTIC SPUR GEAR - HPC ZG1.5-30	1
24	EIF-9-GP-24	PLASTIC SPUR PINION GEAR - HPC ZG1.5-24	1
25	EIF-16-GP-24	PLASTIC COVER	1
26	EIF-2-GP-24	L-PLATE	8
27	EIF-28-GP-24	FRONT GUIDE BUMPER	1
28	EIF-29-GP-24	BACK GUIDE BUMPER	1
29	EIF-32-GP-24	COUNTERSUNK FLAT SCREW - M4 X 6	4

TOLERANCES X = ± 0.5 X.X = ± 0.1 X.XX = ± 0.02		THIRD ANGLE PROJECTION 	MATERIAL: N/A	TITLE: FULL ASSEMBLY	Imperial College London Department of Mechanical Engineering
NAME DRAWN FARHADUL ISLAM CHECKED WENBO CHEN APPROVED RAJIV SAMANTA		DATE 01.11.18 04.11.18 05.11.18	MATERIAL: N/A ALL DIMENSIONS ARE IN MILLIMETRES DO NOT SCALE DRAWING A3 SCALE N/A	DWG No. EIF-31-GP-24	
SHEET 4 OF 4 REVISION 1					